Australian and New Zealand Institutes of Physics

35th Annual Condensed Matter and Materials Meeting

Charles Sturt University, Wagga Wagga, NSW

2nd - 4th February, 2011

CONFERENCE HANDBOOK

WW2011 Organising Committee

Jaan Oitmaa
Chris Hamer
Marion Stevens-Kalceff
Clemens Ulrich
Adam Micolich
Michelle Simmons
Oleg Sushkov
Alex Hamilton

http://www.phys.unsw.edu.au/wagga11

WW2011 CONTENTS

Cover
Scanning tunnelling microscopy based hydrogen lithography allows for the atomically precise patterning of phosphorus dopants in silicon at the sub-nm scale. Using our unique fabrication strategy we have created a single crystal Si:P quantum dot with just 7 donors which are buried below the surface in epitaxial silicon, well away from the presence of any interface traps. As a consequence these devices are extremely stable. We have made electrical transport measurements of this 7 P donor device and find that the atomically abrupt lateral confinement given by the STM patterning breaks the valley splitting in the dot, giving rise to a surprisingly dense excitation spectrum. This work, an important milestone towards single donor devices, was published Nature Nanotechnology (2010)
M.Y. Simmons UNSW

WW2011 MAPS

Wagga Wagga

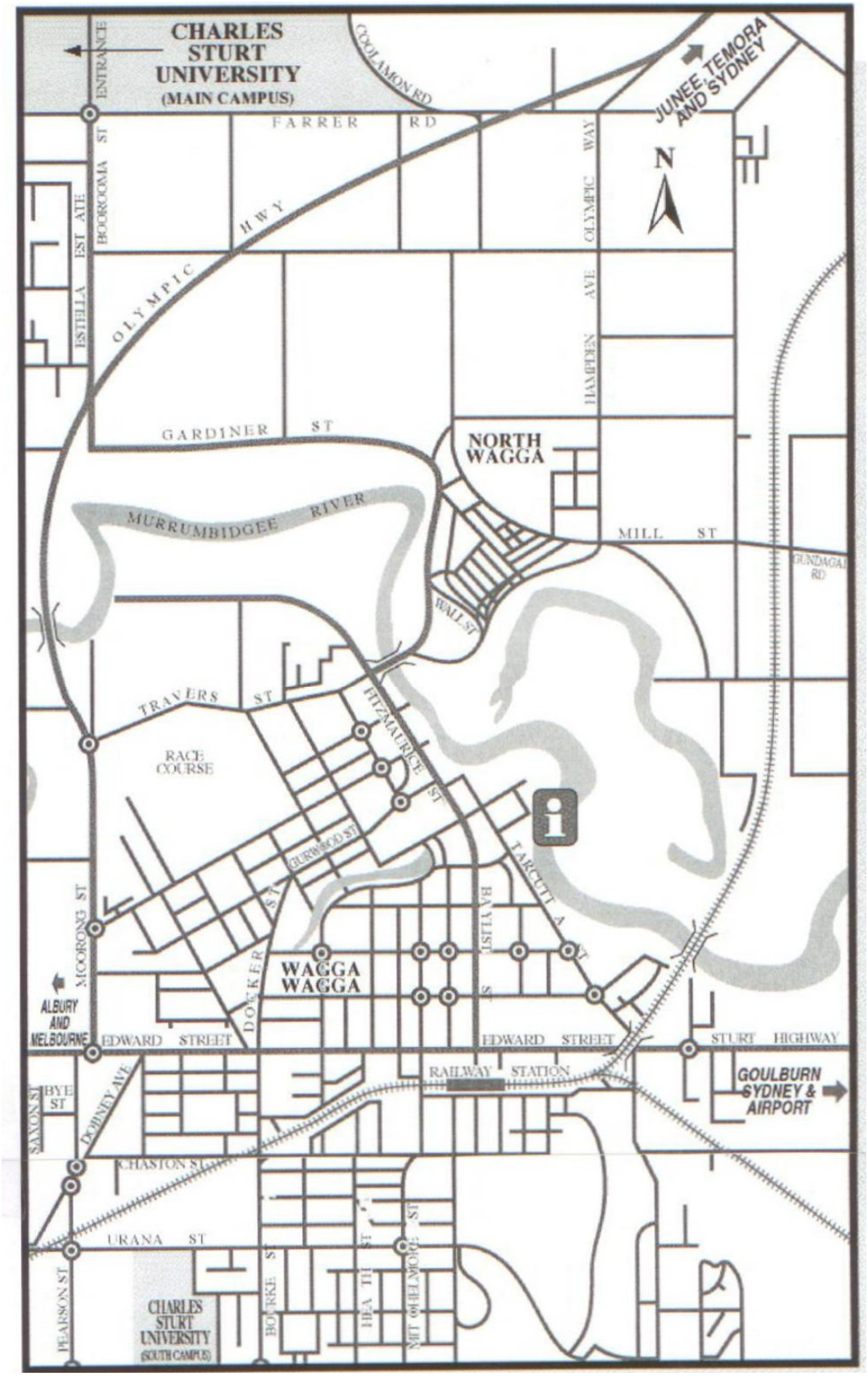

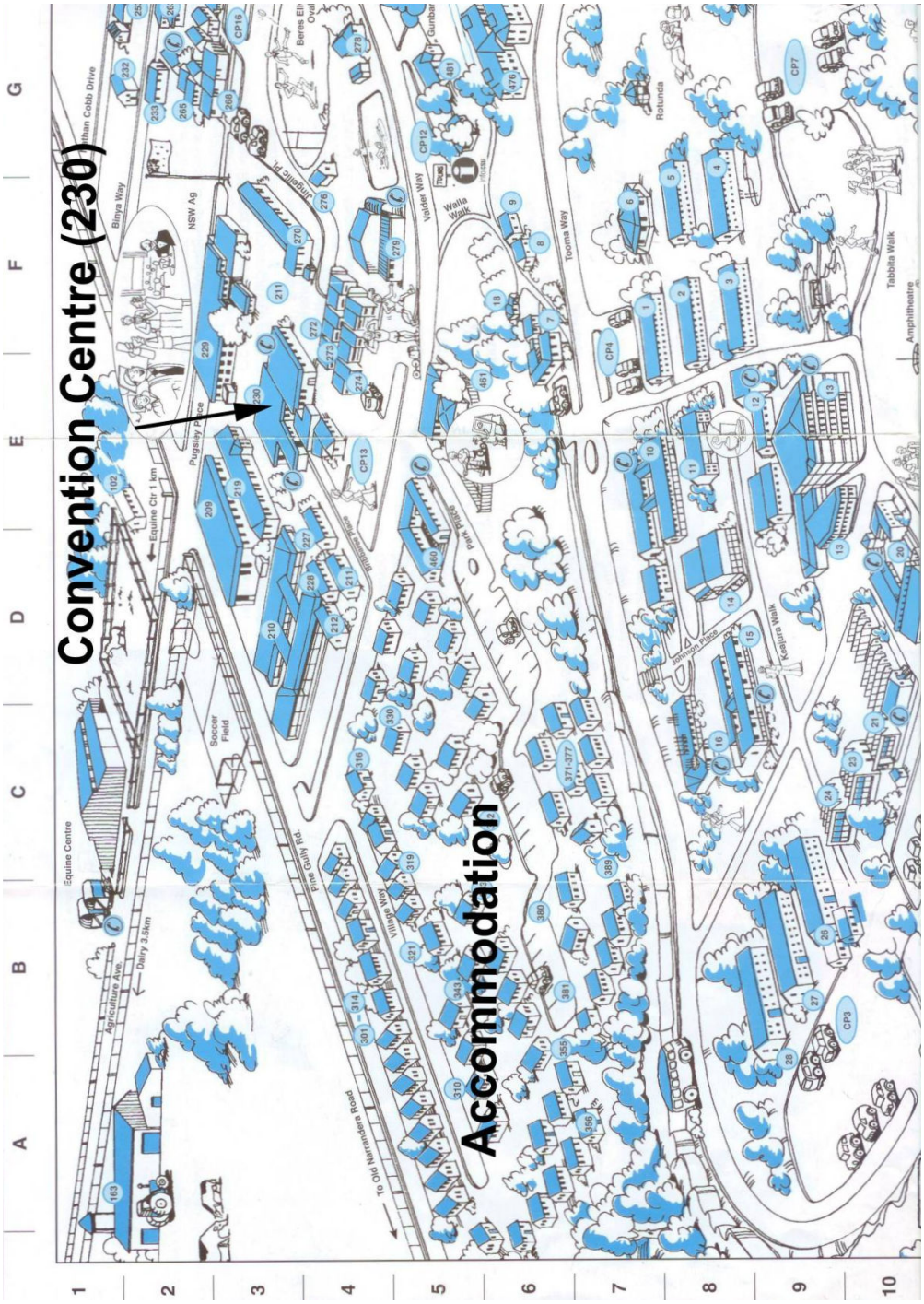
Convention Centre (230)
Accommodation
Equine Centre
Agriculture Ave
Dairy 3.5km
Equine Ctr 1 km
Binya Way
NSW Ag
Pugsley Place
Soccer Field
Prine Gully Rd
To Old Narrandera Road
Walla Walk
Toona Way
Rotunda
Amphitheatre
Tabbita Walk
Kalpura Walk
Johnston Place
CP3
CP4
CP7
CP12
CP13
CP16

WW2011 INFORMATION FOR PARTICIPANTS

Scientific Program:

All poster sessions and lectures will be held at the Convention Centre. Chairpersons and speakers are asked to adhere closely to the schedule for the oral program. A PC laptop computer and data projector, overhead projector, pointer and microphone will be available. Please check that your presentation is compatible with the facilities provided as early as possible. Posters should be mounted as early as possible, and will be displayed on both Wednesday and Thursday. Please remove all posters by Friday morning.

Logistics:

Please wear your name tag at all times. Registration and all other administrative matters should be addressed to the registration desk or a committee member. For lost keys or if locked out of your room from 0900 to 1700, contact Shiralee Hillam at the Events Office for assistance 6933 4974; after hours, contact the Accommodation and Security Office near the corner of Valder Way and Park Way or phone them at 6933 2288. Delegates must check out of their rooms on Friday morning, before 10:00.

Meals, Refreshments and Recreational Facilities:

All meals will be served in the dining room, except the Conference Dinner on Wednesday 7 February, which will be held in the Convention Centre. You will receive a dining room pass on registration and a ticket to the Conference Dinner. The dining room pass must be produced at every meal. It may also be required as identification for use of all other campus facilities, which are at your disposal.

Morning and afternoon tea will be served each day, as indicated in the timetable. Coffee and tea-making facilities are also available in the Common Room of each residence. In addition, on arrival on Tuesday afternoon and for the poster sessions, drinks will be available from the Conference Bar.

The swimming pool is open on weekdays from 06:00 until 21:00, as are the adjacent gymnasium and squash courts. Tennis courts opposite the oval are also available. A wide range of facilities such as exercise bikes, weight training, table tennis and basketball are available in the gymnasium. All of the facilities are free, i.e. covered by your registration fee.

Convention Centre Contact Numbers:

Registration Desk Phone		(02) 6933 4989
Convention Centre Office Phone	(02) 6933 2606	Fax (02) 6933 2643
Events Office Phone		(02) 6933 4974
After hours Emergencies, Accommodation and Security Office Phone		(02) 6933 2288

Internet access: wireless internet access will be available within the Convention Centre (see http://www.csu.edu.au/division/dit/wireless/index.htm)

VV2011 SPONSORS

scitek australia

WARSASH Scientific

JAVAC

STANTON SCIENTIFIC
Vacuum Science Products

Australian Government

ansto
Nuclear-based science benefiting all Australians

CSIRO

SCIENTIA
MANU ET MENTE
UNSW

WW2011 EXHIBITORS

Craig MARSHALL
craig@scitek.com.au

Scitek Australia Pty Limited
Suite 1B, 10-18 Cliff Street
Milsons Point
NSW 2061

ph. 02-9954-1925
email contact@scitek.com.au

Brett Delahunty
brett@warsash.com.au<mailto:brett@warsash.com.au>

WARSASH Scientific Pty Ltd
Unit 7, The Watertower
1 Marian Street Redfern NSW 2016
(adj. to The Australian Technology Park) PO Box 1685 Strawberry Hills NSW 2012 Australia

Tel: + 61 2 93190122
Fax: + 61 2 93182192
Mob: 0428 410 705
http://www.warsash.com.au

participant	affiliation	email
Abiona Adura	ADFA	Adurafimihan.abiona@student.adfa.edu.au
Rose Ahlefeldt	ANU	Rose.ahlefeldt@anu.edu.au
Emma Anderson	ANU	U4350892@anu.edu.au
John Bartholomew	ANU	Jgb111@physics.anu.edu.au
Maciej Bartkowiak	ADFA	Maciej.Bartkowiak@student.adfa.edu.au
Tim Bastow	CSIRO	Tim.bastow@csiro.au
Joel Bertinshaw	ANSTO	Joel.bertinshaw@gmail.com
Susan Biering	Massey	s.b.biering@massey.ac.nz
Jim Boland	CSIRO	jnf_boland@yahoo.com.au
Stewart Campbell	ADFA	Stewart.campbell@adfa.edu.au
John Cashion	Monash	John.cashion@monash.edu
Wei Chen	UNSW	wchen@phys.unsw.edu.au
Stephen Collocott	CSIRO	Stephen.collocott@csiro.au
Evan Constable	Wollongong	Ec028@uowmail.edu.au
David Cookson	Synchrotron	Fran.westmore@synchrotron.org.au
David Cortie	ANSTO	dcr@ansto.gov.au
Michael Cortie	UTS	Michael.cortie@uts.edu.au
Geoff Cousland	Sydney	g.cousland@physics.usyd.edu.au
Paul Dastoor	Newcastle	Paul.Dastoor@newcastle.edu.au
Brett Delahunty	Warsash	Brett@warsash.com.au
M. de Los Reyes	ANSTO	mry@ansto.gov.au
Guodong Du	Wollongong	Gd616@uow.edu.au
John Dunlop	CSIRO	John.viv@optusnet.com.au
Trevor Finlayson	Melbourne	trevorf@unimelb.edu.au
Neville Fletcher	ANU	Neville.fletcher@anu.edu.au
Laura Gladkis	ADFA	l.gladkis@adfa.edu.au
Paul Gubbens	Delft	P.C.M.Gubbens@tudelft.nl
Chris Hamer	UNSW	c.hamer@unsw.edu.au
Steve Harker	ADFA	s.harker@adfa.edu.au
Anita Hill	CSIRO	Anita.hill@csiro.au
Briana Hillman	ANU	U4528TP78@anu.edu.au

Michael Holt	UNSW	mholt@phys.unsw.edu.au
Jessica Hudspeth	ANU	Jessica.hudspeth@anu.edu.au
Wayne Hutchison	ADFA	w.hutchison@adfa.edu.au
Paolo Imperia	ANSTO	plo@ansto.gov.au
C. Jagadish	ANU	Chennupati.jagadish@anu.edu.au
Vedran Jovic	Auckland	jovicvedran@hotmail.com
Bill Kemp	ADFA	w.kemp@adfa.edu.au
Shane Kennedy	ANSTO	sjk@ansto.gov.au
Mustafa Keskin	Erciyes	keskin@erciyes.edu.tr
Hannes Krueger	ANU	Hannes.krueger@anu.edu.au
Yakov Kulik	UNSW	ykulik@phys.unsw.edu.au
Desmond Lau	Melbourne	delau@unimelb.edu.au
Philip Lavers	Wollongong	pel@uow.edu.au
Matthew Lay	CSIRO	Matthew.lay@csiro.au
James Leslie	ANU	U4529451@anu.edu.au
Roger Lewis	Wollongong	roger@uow.edu.au
Qi Li	Wollongong	Ql327@uowmail.edu.au
Tommy Li	UNSW	Tommy.li@student.unsw.edu.au
Klaus-Dieter Liss	ANSTO	kdl@ansto.gov.au
Yanyan Liu	ADFA	Yanyan.liu@adfa.edu.au
John Macfarlane	CSIRO	jcmacfarlane@netspace.net.au
Neil Manson	ANU	Neil.manson@anu.edu.au ?
Jianfeng Mao	Wollongong	Jm975@uow.edu.au
Craig Marshall	Scitek	craig@scitek.com.au
Sara Marzban	ANU	Sara.marzban@anu.edu.au
Garry McIntyre	ANSTO	gmi@ansto.gov.au
Nikhil Medekhar	Monash	Nikhil.medekhar@monash.edu
Peter Metaxas	UWA	Metaxas@physics.uwa.edu.au
Adam Micolich	UNSW	Adam.micolich@gmail.com
Gerard Milburn	UQ	milburn@physics.edu.au
Richard Mole	ANSTO	Richard.mole@ansto.gov.au
Annemieke Mulders	ADFA	a.mulders@adfa.edu.au
Jaan Oitmaa	UNSW	j.oitmaa@unsw.edu.au
Don Price	retired	Don.price@csiro.au
Krunal Radhanpura	Wollongong	Kr965@uowmail.edu.au

Ateeq-ur-Rehman	Zhejiang	Ateeq215@gmail.com
J. Roberts	ANU	Jxr107@physics.anu.edu.au
Lachlan Rogers	ANU	Lachlan.rogers@anu.edu.au
Sven Rogge	UNSW	s.rogge@unsw.edu.au
Jeff Sellar	Monash	Jeff.sellar@monash.edu
Neeraj Sharma	ANSTO	njs@ansto.gov.au
Tilo Soehnel	Auckland	t.soehnel@auckland.ac.nz
Anna Sokolova	ANSTO	Anna.sokolova@ansto.gov.au
Glen Stewart	ADFA	g.stewart@adfa.edu.au
Supitcha Supansomboon	UTS	Supitcha.supansomboon@student.uts.edu.au
Oleg Sushkov	UNSW	sushkov@phys.unsw.edu.au
Jeff Tallon	MacDiarmid	j.tallon@irl.cri.nz
C.J Tang	Sichuan	tchangjian@scu.edu.cn
WenXin Tang	Monash	Wenxin.tang@monash.edu
Gordon Troup	Monash	Gordon.troup@monash.edu
Clemens Ulrich	UNSW	Ulrich@phys.unsw.edu.au
Lou Vance	ANSTO	erv@ansto.gov.au
Jake Warner	ADFA	j.warner@student.adfa.edu.au
Jianli Wang	Wollongong	jianli@uow.edu.au
Ryan Weed	ANU	Ryan.weed@anu.edu.au
Ross Whitfield	ANU	Ross.whitfield@anu.edu.au
Karl Whittle	ANSTO	Karl.whittle@ansto.gov.au
Peng Zhang	Wollongong	Pz898@uowmail.edu.au
Chang-Xig	Monash	Changxi.zheng@monash.edu
Chao Zhong	Wollongong	Cz527@uow.edu.au

scitek australia

Suite 1B, 10-18 Cliff Street
Milsons Point NSW 2061
Toll Free : 1800 023 467

Tel: : 02 9954 1925
Fax : 02 9954 1939
E-mail : contact@scitek.com.au

Web : www.scitek.com.au

Your Partner in Vacuum!

Scitek Australia is an Australian owned company providing technical solutions and services to Research institutes, Universities, Scientific OEM customers and government organisations.

Our products include HV & UHV vacuum pumps, vacuum valves and gauges, leak detectors, mass spectrometers, wafer/thin film coating machines, Cryogenics, Cryo pumps, X-ray diffraction equipment, evaporation & sputtering materials and field portable GCMS.

We have sales, service and spare parts departments supporting our customers' needs. Our team has over 40 years of experience in vacuum technology and scientific instruments.
We also provide consultation and training of our products.

We pride in our products and we believe in providing leading edge technology, innovated product design to our customer with affordable prices.

We service what we sell and we will travel, as necessary, for installation and on site

maintenance and services of all products we sell. Next time you have a need for any vacuum components from O-ring seal to an entire UHV chamber or Mass Spectrometer, think of Scitek.

CALL 1800 023 467

Service offering at a glance

- Fast, competent service
- On site repairs
- Maintenance and repairs at our service centre
- Exchange products and spare parts
- User training for safe, dependable operation
- Custom-tailored service agreements

In-house Services:

- Mass spectrometers (overhaul and testing)
- Turbo molecular pumps
- Vacuum gauge heads
- Leak detectors
- Rotary Vane pumps
- Diaphragm pumps
- Scroll pumps

Onsite Services:

- *Trouble shooting on vacuum systems*
- *Vacuum and pressure helium leak detection*
- *Onsite Training*

Spare Parts

- We offer spare parts for all of our products at competitive prices

Maintenance

- Regular maintenance safeguards against sudden and unexpected failures.
- We can offer Preventative Maintenance and Corrective Maintenance to your needs.

Training

- Training course available on operation and repairs of our Pfeiffer products.

CALL US FOR SERVICE ENQUIRY

02 9954 1925

service@scitek.com.au

Associated Companies

Pfeiffer Vacuum
Products: *Vacuum Pumps (Turbo, Rotary Vane, Dry, Roots pumps) Vacuum Gauges, Leak Detectors, Mass Spectrometers, Valves and Feedthroughs*

VAT Vacuum Valves
Products: *Vacuum valves*

COM VAT
Products: *Welded Bellows*

Anest Iwata
Products: *Dry Scroll Vacuum Pumps*

Huber
Products: *X-ray Diffraction & Positioning Equipment*

UMICORE
Products: *Evaporation & Sputtering Materials*

Austin Scientific
Products: *Cryo pumps, Cryo Cooler*

Advanced Research Systems
Products: *Cryostats*

Applied Thermal control
Products: *Chillers*

EVATEC
Products: *Evaporation, Sputtering , Etch Systems*

Physical Electronics Inc. (PHI)
Products: *XPS, Auger, TOF-SIMS*

Inficon (GC/MS)
Products: *Chemical Identification System-HAPSITE Portable GC/MS*

Inficon (Micro GC)
Products: *Chemical Monitoring System (Micro GC Gas Analyser)*

Inficon (Thickness Monitor)
Products: *Thin Film Deposition Controller*

Oerlikon Optics
Products: *Optical Disc, Data Storage*

Oerlikon Balzers Coating
Products: *Coating Machines*

OVERALL TIMETABLE

Tuesday 1 February

16:00 -	Registration desk open
16:00 – 18:00	*Conference bar open*
18:00 – 19:30	*Dinner*
19:00 -	Posters WP1-WP25 to be mounted

Wednesday 2 February

07:30 – 08:30	*Breakfast*
08:45 – 09:00	Conference opening
09:00 – 10:30	Oral Session: Papers W1 – W3
10:30 – 10:50	*Morning tea*
10:50 – 12:20	Oral Session: Papers W4 – W7
12:20 – 13:30	*Lunch*
13:30 – 14:00	*Break*
14:00 – 15:30	Oral Session: Papers W8 – W11
15:30 – 16:00	*Afternoon Tea*
16:00 – 18:00	Poster Session: Papers WP1 – WP25
19:00 -	Posters TP1 – TP24 to be mounted
16:30 – 18:00	*Conference bar open*
18:30 – 22:00	*Conference Dinner*

Thursday 3 February

07:30 – 08:30	*Breakfast*
09:00 – 10:30	Oral Session: Papers T1 – T4
10:30 – 10:50	*Morning tea*
10:50 – 12:30	Oral Session: Papers T5 – T8
12:20 – 13:30	*Lunch*
14:00 – 15:30	Oral Session: Papers T9 – T12
15:30 – 16:00	*Afternoon Tea*
16:00 – 18:00	Poster Session: TP1 – TP24
16:30 – 18:00	*Conference bar open*
18:00 – 19:00	*Dinner*
20:00 – 22:30	Trivia Quiz (Lindsay Davis Cup)

Friday 4 February

07:30 – 08:30	*Breakfast*
09:00 – 10:30	Oral Session: Papers F1 – F4
10:30 – 10:50	*Morning tea*
10:50 – 12:00	Oral Session: Papers F5 – F7
12:00 – 12:20	Presentations and Closing
12:20 – 13:30	*Lunch*

www.csiro.au

CSIRO Materials Science and Engineering

CSIRO Materials Science and Engineering is focussed on research in manufacturing, health, devices and engineering, materials science and development. Our vision is to deliver great value to Australia by creating world-class innovation in materials science and engineering and to achieve this we are working with a number of leading Australian manufacturing industries.

Much of our innovation in new materials occurs at the intersection of biology, chemistry and physics. Our research here is making an impact in the areas of manufacturing, health, automotive, rail and aerospace, defence, and resource exploration.

Our research areas include:

Surface, Fibre and Protein Chemistry

Advanced biopolymer chemistry combined with expertise in fibre surface science applied to the textile, timber, food packaging and health domains, for example the treatment of fibre surfaces to impart new functionality, such as shrink resistance, stain blocking and improved moisture transport.

Renewable resources from natural timber fibres and polymers for a range of biomaterials and products, including nanostructured materials.

Nanofibrous and Nanostructured Materials

Production and manipulation of nanoscale fibres including the synthesis of carbon nanotubes, electrospinning, processing polymer nanofibres and the extrusion of nanocomposites fibres.

Development of methods for controlling the properties of materials by altering their structure at the nano level, working with a wide range of materials from metals to proteins, with a strong interest in separation technologies.

Biomedical

Application of expertise in nanofibres and bio-compatible polymers to build fibrous scaffolds for the purpose of growing cell cultures to regenerate human tissues.

Thin Film Coatings

Expertise in the physical and chemical properties of thin films, surfaces and structures at the micro- and nano-scale.

Development of hard coatings, particularly nanocomposite coatings containing tiny grains of a material such as titanium nitride in a silicon-based matrix.

Development of biomedical materials such as diamond-like carbon which is hard-wearing, low friction, chemically inert, corrosion resistant and biocompatible.

Surface Coatings

Development of protective coatings to extend the life of critical components.

Finding replacements for highly toxic chromate-based coatings.

Development of self-repairing coatings that are able to autonomously heal damage.

Particulate Materials

Understanding particles – size and distribution, morphology, substrate interface, chemistry.

Use of Cold Spray technology to develop advanced coatings.

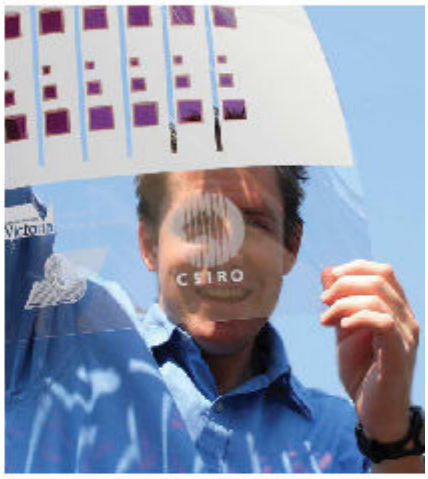

Sensing and Modelling

Development of robust sensors for monitoring atmospheric corrosion; plantar (sole of foot) pressure in patients with peripheral neuropathy; and comfort of patients suffering urinary incontinence.

Nanostructured Materials

Development of methods for controlling the properties of materials by altering their structure at the nano level, working with a wide range of materials from metals to proteins, with a strong interest in separation technologies.

Environmental Catalysis

Development of new catalytic surfaces and membranes with a key focus on helping the environment.

Further Information
contact: Samantha Carroll
phone: (03) 9662 7354
email: sam.carroll@csiro.au
web: www.csiro.au/org/CMSE
www.csiro.au

WW2011 PROGRAM

Tuesday 1 February

16:00 -	Registration desk open
16:00 – 18:00	Conference bar open
18:00 – 19:30	Dinner
19:00 -	Posters WP1-WP25 to be mounted

Wednesday Morning, 2 February

08:45 – 09:00 **Opening: *J. Oitmaa, UNSW***

09:00 – 10:30 **W-I** **Chairperson: *G.A. Stewart, Australian Defense Force Academy***

09:00 – 09:30 W1 100 Years of Superconductivity, 25 Years of HTS *INVITED*
J.L. Tallon, MacDiarmid Institute, Lower Hutt, New Zealand

09:30 – 10:00 W2 Superconductivity: From Zero Resistance to Terahertz Devices
J.C. Macfarlane, CSIRO Materials Science and Engineering

10:00 – 10:30 W3 The Australian Synchrotron and condensed matter science *INVITED*
D.J. Cookson, Australian Synchrotron

10:30 – 10:50 **Morning tea**

10:50 – 12:20 **W-II** **Chairperson: T. Soehnel, University of Auckland**

10:50 – 11:20 W4 Compound Semiconductor Nanowires for Next Generation Optoelectronic Devices *INVITED*
C. Jagadish, The Australian National University

11:20 – 11:40 W5 Terahertz generation from high index GaAs planes at different angles of incidence
K. Radhanpura, University of Wollongong

11:40 – 12:00 W6 Nitrogen Doping and In-situ Heat Treatment of Carbon Nitride Thin Films
D.W.M. Lau, University of Melbourne

12:00 – 12.20 W7 Single dopant transport spectroscopy in silicon
J. Verduijn, S. Rogge, Delft University of Technology, UNSW

12:20 – 14.00 **Lunch**

14:00 – 15:30 **W-III** **Chairperson: *R.A. Lewis, University of Wollongong***

14:00 – 14:30 W8 Engineered quantum systems *INVITED*
G. Milburn, University of Queensland

14:30 – 14:50 W9 Vacancies and Void Formation near Si/SiO_2 Interface
R. Weed, The Australian National University

14:50 – 15:10 W10 Nd-Eu magnetic interactions in Nd^{3+}:$EuCl_3.6H_2O$
R.L. Ahlefeldt, The Australian National University

15:10 – 15:30 W11 Closing the gap: The influence of relativistic effects on the band structure of HgSe and HgTe
S. Biering, Massey University Albany

15:30 – 16:00 **Afternoon Tea**

16:00 – 18:00 **Poster Session: WP1 – WP25**

18:30 – 22:00 **Conference Dinner**

STANTON SCIENTIFIC

Vacuum Science Products

A. & N. Vacuum components
meeting all international standard specifications.
CF, ISO, KF, ASA and other
conventions in the broadest of configurations,
Custom Chambers.

Aalborg Mass Flow Meters and Controllers

Electron Multipliers and Channeltron Detectors

ADVANCED ENERGY
Power Supplies RF and DC
for Thin film deposition , also components and Networks for Plasma loads.

Ion sources and Magnetron sources
For Thin Film , Surface Science and sample preperation applications

HV and UHV feedthroughs
Ceramaseal as used by major instrumentation companies and world class research projects alike.

Granville Phillips Vacuum Gauges

RHK Technology
Imaging the Future of Nanoscience

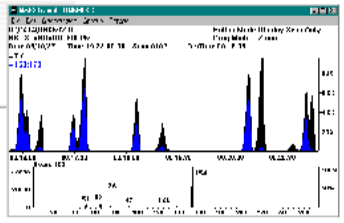

Inficon Thickness Monitors
Quartz Crystal monitoring systems 0.1 Angstrom resolution. Piezo electric valves.

Mass Spectral data bases
N.I.S.T. (USA) and Wiley Mass Spectral Library.

SIMION Ion Optics Software

Diener Plasma Systems

Ion Pumps from Gamma Vacuum

SPECS®
Surface Science
Systems & Components

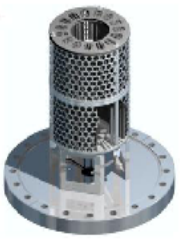

Electron Guns and Power Supplies
from TFI Telemark an established standard in the Field of *Vacuum Deposition* Processes.

www.stantonscientific.com Email : bill@stantonscientific.com

Ph. 02 66856902 Fax 02 85690588

Thursday Morning, 3 February

09:00 – 10:30	**T-I**	**Chairperson: *O.P. Sushkov, UNSW***
09:00 – 09:30	T1	Magnetic domain wall dynamics: from inkblots to spin torque *INVITED* *P.J. Metaxas, University of Western Australia*
09:30 – 09:50	T2	Inelastic Neutron Scattering and EPR Studies of Cobalt Dimers *R.A. Mole, ANSTO, The Bragg Institute*
09:50 – 10:10	T3	Structural and magnetic phase separation in $PrMn_2Ge_{2-x}Si_x$ compounds *J.L. Wang, S.J. Kennedy, University of Wollongong, ANSTO*
10:10 – 10:30	T4	Temperature dependence of the spontaneous remagnetization in $Nd_{60}Fe_{30}Al_{10}$ and $Nd_{60}Fe_{20}Co_{10}Al_{10}$ bulk amorphous ferromagnets *S.J. Collocott, CSIRO Materials Science and Engineering*
10:30 – 10:50		**Morning tea**
10:50 – 12:30	**T-II**	**Chairperson: *K.-D. Liss, The Bragg Institute / ANSTO***
10:50 – 11:20	T5	Engineering graphene growth *INVITED* *N. Medhekar, Monash University*
11:20 – 11:40	T6	101 uses for the nitrogen-vacancy centre in diamond *N. Manson, Australian National University*
11:40 – 12:00	T7	Hard-ball modelling of BCC to closest-packed transition in nanoscale shape memory alloy actuators *M.B. Cortie, University of Technology Sydney*
12:00 – 12.30	T8	Structural variety in brownmillerite-type materials *INVITED* *H. Krüger, The Australian National University, University of Innsbruck*
12:30 – 14.00		**Lunch**
14:00 – 15:30	**T-III**	**Chairperson: *A.J. Hill, CSIRO Materials Science and Engineering***
14:00 – 14:20	T9	The structure of Yttria-Stabilized Zirconia: A combined medium energy photoemission and ab-initio investigation *G. Cousland, The University of Sydney*
14:20 – 14:40	T10	Positron Annihilation Lifetime Spectra of Radiation Damage, Neutral Zircon Crystals *J. Roberts, The Australian National University*
14:40 – 15:00	T11	Experimental study of diffusion and clustering in aluminum alloys *M.D.H. Lay, CSIRO Material Science and Engineering*
15:00 – 15:20	T12	Neutrons and Li-Ion Batteries *N. Sharma, ANSTO, The Bragg Institute*
15:20 – 15:50		**Afternoon Tea**
16:00 – 18:00		**Poster Session: TP1 – TP24**
18:00 – 19:00		**Dinner**
20:00 – 22:30		**Trivia Quiz, Conference Centre** *Quizmaster: Trevor Finlayson, University of Melbourne*

Friday Morning, 4 February

09:00 – 10:30 **F-I** **Chairperson: *S.J. Collocott, CSIRO Materials Science and Engineering***

09:00 – 09:30 F1 Advanced resonant X-ray diffraction applied to the study of ordering phenomena in complex oxides *INVITED*
A.M. Mulders, Australian Defense Force Academy @UNSW

09:30 – 09:50 F2 Cu_5SbO_6 – Synchrotron, Neutron Diffraction Studies and Magnetic Properties
T. Söhnel, The University of Auckland

09:50 – 10:10 F3 Comparison investigation for flux pinning of Titanium and Zirconium doped $Y_1B_2C_3O_{7-\delta}$ films prepared by TFA-MOD
Q. Li, University of Wollongong

10:10 – 10:30 F4 Diffuse scattering from PZN ($PbZn_{1/3}Nb_{2/3}O_3$)
R.E. Whitfield, The Australian National University

10:30 – 10:50 **Morning tea**

10:50 – 12:00 **F-II** **Chairperson: *M.B. Cortie, University of Technology Sydney***

10:50 – 11:20 F5 Multilayered Water-Based Organic Photovoltaics
A. Stapleton, P.C. Dastoor, University of Newcastle *INVITED*

11:20 – 11:40 F6 Study on the interface between organic and inorganic semiconductors
A.-U. Rehman, Zhejiang University, China

11:40 – 12:00 F7 Slow photon photocatalytic enhancement in titania inverse opal photonic crystals
V. Jovic, G.I.N Waterhouse, The University of Auckland, Auckland

12:00 – 12:20 **Presentations and Closing**

12:20 – 14.00 **Lunch**

POSTER SESSION: Wednesday 2 February

(Listed in alphabetical order by first author)

WP1 A.A. Abiona, W.J. Kemp, A.P. Byrne, M. Ridgway, and H. Timmers
Possible Pb-vacancy pairing in germanium: Dependence on doping and orientation

WP2 J.G. Bartholomew, S. Marzban, M.J. Sellars, and R.-P. Wang
Coherence properties of rare earth ion doped thin films

WP3 M. Bartkowiak, G.J. Kearley, M. Yethiraj, and A M Mulders
Ab initio determination of the structure of the ferroelectric phase of $SrTi^{18}O_3$

WP4 T.J. Bastow, C.R. Hutchinson, A. Deschamps, and A.J. Hill
Precipitate growth in a mechanically stressed (deformed) Al(Cu,Li,Mg,Ag) alloy observed by ^{7}Li, ^{27}Al, and ^{63}Cu NMR and XRD

WP5 J. Bertinshaw, T. Saerbeck, A. Nelson, M. James, V. Nagarajan, F.Klose, and C. Ulrich
Studying multiferroic $BiFeO_3$ and ferromagnetic $La_{0.67}Sr_{0.33}MnO_3$ tunnel junctions with Raman spectroscopy and neutron scattering techniques

WP6 J.D. Cashion, W.P. Gates, T.L. Greaves, and O. Dorjkhaidav
Identification of Fe^{3+} site coordinations in NAu-2 Nontronite

WP7 W. Chen and O.P. Sushkov
Fermi arc – hole pocket dichotomy: effect of spin fluctuation in underdoped cuprates

WP8 E. Constable and R.A. Lewis
Continuous-wave terahertz spectroscopy as a non-contact, non-destructive method for characterising semiconductors

WP9 M. de los Reyes, K.R. Whittle, M. Mitchell, S.E. Ashbrook, and G.R Lumpkin
Pyrochlore-fluorite transition in $Y_2Sn_{2-x}Zr_xO_7$ - implications for stability

WP10 B. Deviren, S. Akbudak, and M. Keskin
Mixed spin-1 and spin-3/2 Ising system with two alternative layers of a honeycomb lattice within the effective-field theory

WP11 J.B. Dunlop, T.R. Finlayson, and P. Gwan
Condensed matter and materials trivia

WP12 C. Feng, H. Li, G. Du, Z. Guo, N. Sharma, V.K. Peterson, and H. Liu
Non-stoichiometric Mn doping in olivine lithium iron phosphate: structure and electrochemical properties

WP13 T.R. Finlayson, S. Danilkin, A.J. Studer, and R.E. Whitfield
Anomalous precursive behaviour for the martensitic material $Ni_{0.625}Al_{0.375}$

WP14 L.G. Gladkis, H. Timmers, J.M. Scarvell, P.N. Smith
Reliable shape information on prosthesis wear debris particles from atomic force microscopy

WP15 C.J. Hamer, O. Rojas, and J. Oitmaa
A frustrated 3D antiferromagnet: stacked J_1-J_2 layers

WP16 S.J. Harker, H. Okimoto, G.A. Stewart, K. Nishimura, and W.D. Hutchison
An ^{57}Fe-Mossbauer study of the magnetic phase diagram for $Nb_{1-x}Hf_xFe_2$

WP17 B. Hillman, D. James, J. Dong, W.D. Hutchison, D.J. Goossens
Magnetic and structural properties of some compounds in the MM'PS3 family

WP18 M. Holt and O.P. Sushkov
Mobile hole dynamics in the vicinity of an O(3) quantum critical point

WP19 J.M. Hudspeth, D.J. Goossens, and T.R. Welberry
Modelling short-range order in triglycine sulphate

WP20 W.D. Hutchison, P.G. Spizzirri, F. Hoehne, L.Y.S. Soo, L.K. Alexander, and M.S. Brandt
Studies of near surface phosphorus donors in silicon via electrically detected magnetic resonance

WP21 P. Imperia
New sample environments and science opportunities at the Bragg Institute

WP22 W.J Kemp, A.A. Abiona, P. Kessler, R. Vianden, H. Timmers
Time differential perturbed angular correlation spectroscopy of ^{100}Pd/Rh in Rhenium and Hafnium

WP23 M. Koeberle, E. Pogson, R. Jakoby and R. A. Lewis
Characterization of Nematic Liquid Crystals using Terahertz spectroscopy

WP24 Y. Kulik and O.P. Sushkov
Decay width of longitudinal magnon in the vicinity of an O(3) quantum critical point

WP25 P.S. Lavers
Topological atoms in crystals and their role in crystalline bonds

POSTER SESSION: Thursday 3 February

TP1 J. Leslie, B. Hillman, and P. Kluth
Proximity effect on ion track etching in amorphous SiO_2

TP2 T. Li, O.P. Sushkov, and U. Zuelicke
Spin dynamics and Zeeman splitting of holes in a GaAs point contact

TP3 K.-D. Liss, D.D. Qu, M. Reid, and J. Shen
On the atomic anisotropy of thermal expansion in bulk metallic glass

TP4 Y. Liu and H. Timmers
Possible lubrication and temperature effects in the microscratching of polyethylene terephthalate

TP5 A. E. Malik, W.D. Hutchison, K. Nishimura, and R.G. Elliman
Studies of magnetic nanoparticles formed in SiO_2 by ion implantation

TP6 J. Mao, Z. Guo, and H. Liu
Effect of hydrogen back pressure on de/rehydrogenation behaviour of $LiBH_4$-MgH_2 system and the role of additive toward to enhanced hydrogen sorption properties

TP7 A.P. Micolich, K. Storm, G. Nylund, and L. Samuelson
Chemical control of gate length in lateral wrap-gated InAs nanowire FETs

TP8 J. Oitmaa and A. Brooks Harris
High temperature thermodynamics of the multiferroic $Ni_3V_2O_8$

TP9 J. Oitmaa and C.J. Hamer,
Does the quantum compass model in 3D have a phase transition?

TP10 J. Oitmaa and O.P. Sushkov
Scaling of critical temperature and ground state magnetization near a quantum phase transition

TP11 L.J. Rogers, K.R. Ferguson, and N.B. Manson
Strain to selectively excite certain orientations of NV centres in diamond

TP12 S. Sakarya, P.C.M. Gubbens, A. Yaouanc, P. Dalmas de R´eotier, D. Andreica, A. Amato, U. Zimmermann, N. H. van Dijk, E. Brück, Y. Huang, T. Gortenmulder, A. D. Hillier, and P. J. C. King
Ambient and high pressure μSR measurements on the ferromagnetic superconductor UGe_2

TP13 A. Sokolova
Small Angle Scattering: instrumentation and applications to study various materials at the nanoscale

TP14 G.A. Stewart, H. Salama, A. Mulders, D. Scott, and H.StC. O'Neill
Thermal hysteresis of the ^{169}Tm quadrupole interaction in orthorhombic thulium manganite

TP15 S. Supansomboon, A. Dowd, and M.B. Cortie
Phase relationships in the $PtAl_2$-$AuA1_2$ system

TP16 W. X. Tang, C. X. Zheng, Z. Y. Zhou, D. E. Jesson, J. Tersoff
Surface dynamics during Langmuir evaporation of GaAs

TP17 G.J.Troup, D.R.Hutton, J.Boas, A.Casini, M.Picollo, and Robyn Slogget
From radiation damage, through minerals and gemstones, to art with EPR

TP18 J.L. Wang, A.J. Studer, S.J. Campbell, S.J. Kennedy, R. Zeng, and S.X. Dou
Magnetic structures of $Pr_{1-x}Lu_xMn_2Ge_2$ compounds (x = 0.2 and 0.4)

TP19 J.A. Warner, L.G. Gladkis, A. E. Kiss, J. Young P.N. Smith, J. Scarvell, and H.Timmers
Polymer particle production and dispersion in Knee prostheses

TP20 K.R. Whittle, D.P. Riley, M.G. Blackford, R.D. Aughterson, S. Moricca, G.R. Lumpkin, and N.J. Zaluzec
$M_{(n+1)}Ax_n$ Phases are they tolerant/resistant to damage

TP21 W. Xie, H. Ju, J.I. Mardel, A.J. Hill, J.E. McGrath, and B.D. Freeman
The role of free volume in the tradeoff between high water permeability and high permeability selectivity of polymeric desalination membranes

TP22 P. Zhang, Z. Guo, and H. Liu
Electrospinning technology used to synthesize nanomaterials for lithium ion batteries

TP23 C.X. Zheng, Z.Y. Zhou, W.X. Tang, D.E. Jesson, J. Tersoff, and B. A. Joyce
Design and application of a III-V surface electron microscope

TP24 C. Zhong, J.Z. Wang, S.L. Chou, K. Konstantinov and H.K. Liu
Spray pyrolysis prepared hollow spherical CuO/C: synthesis, characterization, and its application in lithium-ion batteries

WW2011 ABSTRACTS FOR ORAL SESSIONS

W1

100 years of superconductivity, 25 years of HTS

J.L. Tallon

MacDiarmid Institute for Advanced Materials and Nanotechnology, Industrial Research Ltd, P.O. Box 31310, Lower Hutt, New Zeland.

This year it's a century since the discovery of superconductivity and a quarter of a century since the discovery of high-T_c superconductors (HTS). The initial hype was perhaps overstated but, already, HTS are overtaking LTS in a broad suite of applications which I will describe [1]. But do we understand them? It took 46 years to develop a theory of low-T_c superconductivity (LTS) so it is perhaps not too surprising that we still don't know how HTS work. Nonetheless, I will show that we do understand a great deal about HTS and that the basic rules of design can be determined from studying their systematics. In fact we know how to design the ideal HTS superconductor. This in turn, in this International Year of Chemistry, lays down a challenge for the chemist. Can the ideal design be synthesised? Progress may seem slow, but this field will continue to thrive over the next few decades because there is much more scope for (i) fascinating science, (ii) improved performance and (iii) escalating commercialisation.

J.L. Tallon and R.G.Buckley, *The Discovery and Development of High-T_c Supercon-ductors*, book chapter to appear in *New Zealand is Different*, Vol. 2, ed by Bryce Williamson. (2011).

W2

Superconductivity : From Zero Resistance to Terahertz Devices

J.C. Macfarlane[a], J.Du[a] and C.M Pegrum[b]

[a] *CSIRO Materials Science and Engineering, NSW 2070, Australia.*

[b] *Strathclyde University, Glasgow, G4 0NG, UK.*

The evolution of work on the unique phenomena of superconductivity has generated a broad diversity of research in electronic/electromagnetic applications, very few of which are based on the original property of zero-resistance that was discovered by Kamerlingh Onnes [1] in 1911. The more subtle, but powerful, macroscopic quantum phenomena arising from the quantization of magnetic flux and the Josephson effects [2] have proved to be a much richer field for the growth and study of new device physics. Here I attempt to present a brief survey of a number of significant applications that have emerged from work on electrotechnology in the 1970s and now extend across the electromagnetic spectrum, from minerals exploration and sub-ocean surveying, through geo-archaeometry, magneto-encephalography, telecommunications, and THz remote sensing, to the detection of single photons for radio astronomy and single fluxons for quantum information.

[1] "The Cold Wars", J. Matricon and G. Waysand, Rutgers U. Press, 2003.

[2] "The SQUID Handbook- Applications of SQUIDs and SQUID Systems". John Clarke and Alex Braginski, Wiley-VCH 2006.

W3

The Australian Synchrotron and condensed matter science

D.J. Cookson, I. Gentle, A. Peele

Science Management

Australian Synchrotron

The Australian Synchrotron (AS) is a world-class resource for cutting edge science and technology. Capable of being used by many different research groups simultaneously, it produces beams of very bright polarised light used to probe matter down to the nanoscale.

Condensed matter science has benefited from technology originally developed for research in high energy physics. At the Australian Synchrotron researchers in nanotechnology, novel materials, crystallography and x-ray imaging have been publishing data collected at this facility since its opening in 2007.

Some of the most recent developments at the Australian Synchrotron will be discussed, along with examples of how this facility is adding value to the condensed matter disciplines.

W4

Compound Semiconductor Nanowires for Next Generation Optoelectronic devices

C. Jagadish

Department of Electronic Materials Engineering, Research School of Physics and Engineering, The Australian National University, Canberra, ACT 0200, Australia

Email: Chennupati.Jagadish@anu.edu.au

III-V compound semiconductor nanowires (NWs) grown via vapor-liquid-solid (VLS) mechanism often exhibit several problems: for example, tapered morphology, high density of planar defects, mixed wurtzite (WZ) and zinc blende (ZB) crystal structures. These problems have to be solved before the commercial device applications for nanowires. In this talk, I will present the research activities in our group at ANU to tackle these problems. Results have shown great success in improving morphology, crystal quality and photoluminescence efficiency.

We demonstrated that GaAs nanowires of high optical and crystal quality may be achieved by choosing an appropriate V/III together with growth temperature. By designing and growing a core-shell GaAs/AlGaAs/GaAs nanowire heterostructure, nearly intrinsic exciton lifetimes (~1 ns) were obtained in these core-shell nanowires, which are comparable to high quality two-dimensional double heterostructures.

We were able to achieve InP nanowires either in ZB crystal or WZ crystal phase or mixed phases of ZB/WZ structures in a single InP nanowire. Time resolved photoluminescence measurements have shown a type II band alignment in these ZB/WZ mixed phase nanowires and extremely long carrier lifetime (~6400 ps).

In the case of InAs, pure ZB nanowires, free of twin defects, were achieved using a low growth temperature coupled with a high V/III ratio. Conversely, a high growth temperature coupled with a low V/III ratio produced pure WZ nanowires free of stacking faults. This ability to tune crystal structure between twin-free ZB and stacking-fault-free WZ not only will enhance the performance of nanowire devices but also opens new possibilities for engineering nanowire devices, without restrictions on nanowire diameters or doping.

Acknowledgments: This research is supported by the Australian Research Council and Australian National Fabrication Facility established under Australian Government NCRIS Program.

W5

Terahertz generation from high index GaAs planes at different angles of incidence

K. Radhanpura, S. Hargreaves and R. A. Lewis
Institute for Superconducting and Electronics Materials, University of Wollongong, Wollongong, New South Wales 2522, Australia.

Generation of terahertz (THz) radiation from high index GaAs (11N) semiconductor faces, with N ranging from 0 to 5, has been measured using terahertz time domain spectroscopy. The mechanism involved in THz generation in the absence of any external bias may be attributed to either linear transient current (TC) effect or a nonlinear optical rectification (OR) effect. In the case of normal incidence of the near-infrared (NIR) beam on the GaAs emitter, the THz is generated due to optical rectification (OR) only. The theory for the second order bulk OR and third order surface-electric-field induced OR has been represented for any arbitrary indices zinc-blende crystal. By comparing the experimental results with the theory, it can be shown that both bulk and surface OR are responsible for the THz generation from GaAs crystals in transmission geometry [1, 2].

In the case of non-normal incidence of NIR on GaAs emitter, in addition to OR effect, transient current also plays a role in THz generation due to a component of the surface field along the direction of detection. For this quasi-reflection geometry, it has been shown from the theory that the surface OR is in phase with bulk OR for GaAs A face (Ga rich face) and out of phase for B face (As rich face). Hence the overall signal is reduced for B face compared to A face.

S. Hargreaves, K. Radhanpura and R. A. Lewis, *Physical Review B* **80**, 195323 (2009).
K. Radhanpura, S. Hargreaves and R. A. Lewis, *Applied Physics Letters* **94**, 251115 (2009).

W6

Nitrogen Doping and *In-situ* Heat Treatment of Carbon Nitride Thin Films

D.W.M. Lau[a], A.Z. Sadek[b], A. Moafi[b] and D.G. McCulloch[b]

[a] *School of Physics, University of Melbourne, Victoria 3010, Australia.*

[b] *Applied Physics , School of Applied Sciences, RMIT University, GPO Bo 2476V, Melbourne, Victoria 3001, Australia*.

The doping of nitrogen of carbon thin films to tune their electronic properties have been extensively investigated due to their potential applications such as field emission displays [1]. The study of the effect of nitrogen content, post-deposition annealing on microstructure and bonding have been well established [2-4]. However, carbon films deposited with *in-stiu* heat treatment at different ion energies has received little attention. In this paper, we will present results of nitrogen doped carbon films deposited by filtered cathodic arc. Many of the films studied contain oriented graphene sheets perpendicular to the substrate surface [5]. The controlled doping of large uniform graphene sheets is a paramount in exploiting graphene as an electronic/spin material. The films were characterized by X-ray Absorption Spectroscopy (XAS) and Electron Energy Loss Spectroscopy (EELS) which are complementary techniques to probe the inner shell adsorption and hence bonding in these materials. The microstructures of these materials were investigated using TEM.

[1] Z. Shpilman *et al.*, App. Phys. Lett. **89**, 252114 (2006).

[2] S. Bhattacharyya *et al.*, Diamond Rel. Mater. **11**, 8 (2002).

[3] A. C. Ferrari, S. E. Rodil, and J. Robertson, Phys. Rev. B **67**, 155306 (2003).

[4] S. S. Roy *et al.*, Diamond Rel. Mater. **13**, 1459 (2004).

[5] D. W. M. Lau *et al.*, Phys. Rev. Lett. **100**, 176101 (2008).

W7

Single dopant transport spectroscopy in silicon

J. Verduijn[a], G.P. Lansbergen[a], G.C. Tettamanzi[a], R. Rahman[b], S. Biesemans[c], N. Colleart[c], G. Klimeck[d], L.C.L. Hollenberg[d], and S. Rogge[a]

[a] *Kavli Institute of Nanoscience, Delft University of Technology, Delft, The Netherlands.*

[b] *Network for Computational Nanotechnology, Purdue University, USA.*

[c] *InterUniversity Microelectronics Center (IMEC), Kapeldreef 75, 3001 Leuven, Belgium*

[d] *Center for Quantum Computer Technology, University of Melbourne, Australia*

Technology reached a level of miniaturization where we can realize transport through a single dopant atom in a transistor [1]. Such transport spectroscopy can probe the atomic orbitals and the interaction of the atom with the environment [2]. This interaction with the environment in a nano-device alters the dopants properties, such as the level spectrum and the charging energy, from those of the bulk. The system discussed here is a gated arsenic donor in a silicon field effect transistor. Electronic control over the wavefunction of dopants is one of the key elements of quantum electronics. This talk focuses on the role of the restricted momentum space, which has a severe impact on the charge and spin configuration of a donor atom in a nano-device. The combined experimental and theoretical study of the gated two-electron state of the donor led to the realization of the pseudo spin nature of the valleys. We observe a blocked electronic relaxation due to combined spin and valley selection rules. Time averaged transport measurements put a lower bound of 50 ns on the rate of the blocked transition, 1000 times slower than a bulk transition [3]. For the low lying excited states Hund's rule is violated due to vanishing exchange in orthogonal valleys. Furthermore, we observe reduced charging energies and bound singlet and triplet excited states for this negatively charged donor that can be explained in the self consistent tight binding model. Finally, experiments demonstrating coherent coupling between two donors will be discussed [4].

[1] Sellier et al. "Transport spectroscopy of a single dopant in a gated silicon nanowire" PRL 97, 206805 (2006)

[2] Lansbergen et al. "Quantum confinement and symmetry transition of a single gated donor electron in silicon", Nature Physics 4, 656 (2008)

[3] Lansbergen et al. "Vanishing exchange and the emergence of a pseudo-spin in restricted momentum space multi-electron atoms" arXiv:1008.1381

[4] Lansbergen et al. "Tunable Kondo effect on a single donor atom" Nano Letters 10, 455 (2010) & Verduijn et al. "Coherent transport through a double donor system in silicon" APL 96, 043107 (2010)

W8

Engineered Quantum Systems

G.J. Milburn

School of Mathematics and Physics, University of Queensland, QLD 4072, Australia.

Driven by advances in technology and experimental capability, it is now possible to engineer complex multi-component systems that merge the once distinct fields of quantum optics and condensed matter physics. These systems find applications in quantum metrology and quantum information and provide a path to explore the shady world at the quantum classical boundary. A characteristic feature of engineered quantum systems is a description in terms of an effective quantum theory of collective macroscopic variables that largely factor out the microscopic degrees of freedom. This opens up new domains for quantum control enabling quantum machines of increasing size and complexity. I will give an overview of this new field and discuss some specific models and recent experiments, including examples drawn from nanomechanics with superconducting transducers and optomechanics with single photons. I will also give a brief summary of the central research programs in the ARC Centre of Excellence in Engineered Quantum Systems.

W9

Vacancies and Void formation Near Si/Si02 Interface

Ryan Weed a, Simon Ruffell b. James Sullivan a, Steve Buckman a, Andy Knights c

a Centre for Anti·Matter Matter Studies. Research School of Physics and Engineering Australian National University, Canberra 0200 Australia

b Department of Electronics Materials Engineering. Research School of Physics and Engineering Australian National University. Canberra 0200 Australia

c Department or Engineering Physics McMaster University, Hamilton. ON. Canada

The Si/SiO_2 interface is an example of two materials with different lattice constants and structure being brought together to form a surprisingly high quality (few monolayer disorder) interface. The properties of this interface are a key element in the modern electronics revolution. In recent years, much interest has developed toward the study of large vacancy clusters/voids and their utility in silicon device technology. Not only do these voids provide a deep level in the Si band gap, but it has been shown that the void internal surfaces interact strongly with interstitials and vacancies and subsequently have an effect on dopant diffusivity and secondary defect suppression [1, 2]. A more detailed understanding is required of the basic mechanisms of void formation near interfaces and their effect on electrical properties of the semiconductor.

Silicon-on-insulator (SOI) wafers (used in high performance CMOS devices) were chemically etched to provide Si layers of 1 to 2 μm thickness on top of the buried SiO_2. Implantation of He was performed at energies ranging from 100 to 250 keV at various fluences. The combination of implant energy and Si layer thickness allows control of the position of He from the Si surface and the Si/SiO_2 interface. Subsequent annealing at 600 to 800 °C induces void formation through evolution of the implanted He and associated implantation damage. Rutherford backscattering spectroscopy (RBS) was performed in order to verify the silicon layer thicknesses and assess the ion-implantation induced damage.

The Positron Annihilation Lifetime Spectroscopy (PALS) beamline at the Centre for Antimatter-Matter Studies (CAMS) was used to probe the void concentration and size of the voids near the Si/SiO_2 interface. Initial results suggest that the interface acts to inhibit large void formation, and that vacancies and vacancy clusters migrate towards the interface during the annealing procedure.

[1] S.M. Myers and G.A. Petersen, *Transport and reactions of gold in silicon containing cavities* Phys. Rev. B **57,** 7015 (1998).

[2] V. Raineri and S.U. Campisano, *Secondary defect dissolution by voids in silicon* (Applied Physics Letters, 2000) p 1783-1785.

W10

Nd-Eu magnetic interactions in Nd^{3+}:$EuCl_3.6H_2O$

R. L. Ahlefeldt[a], W. D. Hutchison[b] and M. J. Sellars[a]

Laser Physics Centre, Research School of Physics and Engineering, The Australian National University, Canberra 0200, Australia

School of Physical, Environmental and Mathematical Sciences, The University of New South Wales, Australian Defence Force Academy, Canberra, 2600, Australia

$EuCl_3.6H_2O$ is a crystal of interest for quantum information applications because of its high absorption and small optical linewidth. In particular, a quantum system suitable for quantum computing demonstrations could be created in a $EuCl_3.6H_2O$ crystal doped with Nd^{3+}. Europium sites around an Nd^{3+} dopant are strained due to the different radius of Nd^{3+} and this results in satellite lines in the spectrum of the Eu^{3+} $^7F_0$-$^5D_0$ optical transition. Quantum computing gate operations could be performed using interactions between these satellite lines. To do this it is necessary to first associate each satellite line with a crystallographic Eu^{3+} site. The electron spin of the Nd^{3+} ion causes a Zeeman splitting of the hyperfine levels of surrounding Eu^{3+} ions that is different for each satellite line. To associate lines with sites, the Zeeman splitting on the 29 MHz ground state hyperfine transition of Eu^{3+} was recorded for each satellite line as a magnetic field was rotated about the sample. The resulting rotation patterns were modeled using knowledge of the spin Hamiltonian of undoped $EuCl_3.6H_2O$[1] and EPR measurements of the Nd^{3+} Hamiltonian[2], to determine the Eu^{3+}-Nd^{3+} dipole-dipole interaction and hence the ion position.

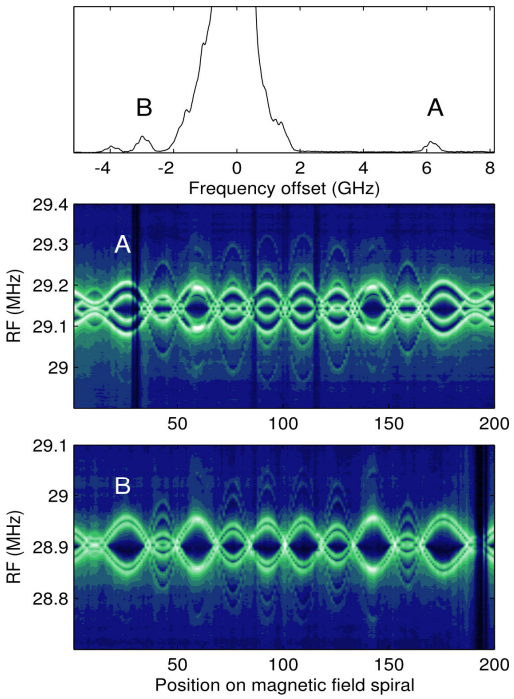

Figure 1. Top: excitation spectrum of the $^7F_0$-$^5D_0$ transition. Bottom: rotation patterns for two satellite lines. The magnetic field is rotated in a spiral covering a sphere.

[1] J. Longdell, A. Alexander and M. Sellars, *Phys. Rev. B.* **74**, 195101 (2006)

[2] M. Schulz and C. Jeffries, *Phys. Rev.* **149**, 270 (1966)

W11

Closing the gap: The influence of relativistic effects on the band structure of HgSe and HgTe

Susan Biering, P. Schwerdtfeger

Centre for Theoretical Chemistry and Physics, The New Zealand Institute for Advanced Study, Massey University Albany, Private Bag 102904, North Shore City, 0745 Auckland , New Zealand.

At ambient pressure, mercury oxide and sulphide in their solid state crystallize in rather unusual chain-like structures, namely montroydite and cinnabar. The sophisticated structures significantly differ from those found for the lighter group 12 chalcogenides ZnX and CdX (X=O, S), which under ambient conditions are known to form comparably simple hexagonal wurtzite and cubic rocksalt or zinc blende structures. Following the periodic table, these structural differences are less pronounced for the selenides and tellurides. However, in the II-VI compound semiconductors, HgSe and HgTe are exceptional with respect to their electronic properties. In stark contrast to the related zinc and cadmium based compounds, they show a semimetallic behaviour and an inverted band structure.

A recent density functional study has shown that relativistic effects play a crucial role in the explanation and understanding of the chain-like structures so typical to mercury chalcogenides, in contrast to the lighter group 12 chalcogenides [1]. Motivated by those findings, the question arises, whether the peculiar electronic properties of HgSe and HgTe can also be attributed to the influence of relativistic effects.

To this end, relativistic, including spin-orbit effects, as well as nonrelativistic density functional studies of the equilibrium phases of ZnX, CdX and HgX (X=O, S, Se, Te) were carried out. It is shown that in mercury selenide and telluride the neglect of relativity goes as far as to change the experimentally observed semimetallic behaviour to the restoration of semiconducting properties.

[1] S. Biering, A. Hermann and P. Schwerdtfeger, *J. Phys. Chem. A* **113**, 12427 (2009).

T1

Magnetic domain wall dynamics: from inkblots to spin torque

P.J. Metaxas

School of Physics, University of Western Australia, Crawley WA 6009, Australia
Unité Mixte de Physique CNRS/Thales, Palaiseau 91767, France

The dynamics of magnetic domain walls continue to attract interest from the international scientific community, not only in view of next generation data storage and data processing technologies [1] but also for the insight that they offer in terms of probing fundamental processes such as spin transfer torque and interface motion. I will give a brief overview of current challenges and research trends in the field of domain wall dynamics as well as present some of our recent experimental results.

The most recent of these is concerned with spin torque: wherein a rf current injected into a magnetic nanostrip is used to resonantly excite a pinned domain wall, thereby facilitating its "depinning" [2]. The majority of presented results however concern domain wall dynamics in ultrathin ferromagnetic Pt/Co/Pt layers which are excellent experimental realisations of 2D weakly disordered Ising systems. Domain walls in these films are essentially unidimensional interfaces and their interaction with structural defects (as well as the consequences for the wall dynamics) can be understood using general theories for interface dynamics. The versatility of magnetic systems has allowed us to experimentally examine these rich interface dynamics not only in the presence of weak structural disorder but also under the influence of periodic pinning potentials [3]. Additionally, from measurements of dynamics in coupled magnetic layers, we have also been able to evidence domain walls in physically separate layers moving together in bound states [4].

Parkin et al, *Science* **320**, 190 (2008); Allwood et al, *Science* **309**, 1688 (2005).
Metaxas et al, *Appl. Phys. Lett.* **97**, 182506 (2010).
Metaxas et al, *Phys. Rev. Lett.* **99**, 217208 (2007); *Appl. Phys. Lett.* **94**, 132504 (2009).
Metaxas et al, *Phys. Rev. Lett.* **104**, 237206 (2010).

T2

Inelastic Neutron Scattering and EPR Studies of Cobalt Dimers

R.A. Mole[a], A. Boeer[b], G. Simeoni,[c] D. Collison[b], E. McInnes[b], G.A. Timco[b] and R.E. P. Winpenny[b]

[a] *The Bragg Institute, Australian Nuclear Science and Technology Organsiation, PMB 1, Menai, NSW, Australia.*

[b] *School of Chemistry, The University of Manchester, Oxford Road, Manchester, M13 9PL, United Kingdom.*

[c] *Forshungsneutronenquelle Heinz Maier-Leibnitz, Technische Universitaet Muenchen, Garching, 85747, Germany*

The phenomenon of single molecule magnetism has been known for over fifteen years and the fundamentals of this behaviour are well understood; the observed hysteresis is due to an energy barrier for spin reversal, the magnitude of this energy barrier is given by the magnitude and anisotropy of the molecular spin. Despite intensive research it has not been possible to improve the performance of the best single molecule magnets to obtain operating temperatures above a few Kelvin. Recent work has suggested that the anisotropy parameter might play a more important role than previously thought. As such clusters consisting of octahedral Co(II) are promising candidates due to the large anisotropy associated with the spin orbit coupling of the $^4T_{1g}$ ground term. There are however no clear cut cobalt single molecule magnets and the magnetic properties of coordination clusters consisting of octahedral cobalt (II) ions are often complex. Here I present an inelastic neutron scattering study of two cobalt dimers $Co_2(D_2O)(L)_4(HL)_2(C_5D_5N)_2$ and $Co_2(D_2O)L_4(HL)_4$ where L = $(CD_3)_3Co_2H$ [1]. These dimers share a common core; though display different bulk magnetic properties. The dimer was chosen as it is the simplest possible exchange coupled unit that can be studied. The use of inelastic scattering for this problem is incredibly powerful, both due to the zero field nature of the technique and the flexible selection rules [2]. The INS data is presented together with the results of multiple frequency EPR and bulk magnetic properties. The complimentary nature of these techniques allows both the energy scale and the ground state to be determined.

[1]: R.E.P. Winpenny *et. al. Chem. Eur.J.,* 9 (2003) 5142
[2]: A. Furrer, H.U. Güdel, *Phys. Rev. Lett.*, 39 (1997) 657

T3

Structural and magnetic phase separation in $PrMn_2Ge_{2-x}Si_x$ compounds

J. L. Wang[a,b,c], S. J. Kennedy[b], S. J. Campbell[c], M. Hofmann[d], , R. Zeng[a],
S. X. Dou[a], A. Arulraj[e] and N. Stusser[e]

[a]*ISEM, University of Wollongong, NSW 2522,*

[b]*Bragg Institute, ANSTO, Lucas Heights, NSW 2234,*

[c]*School of Physical, Environmental and Mathematical Sciences, UNSW@ADFA, ACT 2600*

[d]*FRM-II, Technische Universität München, 85747 Garching, Germany*

[e]*BENSC, Hahn-Meitner Institute, Glienicker Strasse 100, D-14109 Berlin-Wannsee, Germany*

Ternary intermetallic compounds of RMn_2X_2 (where R = rare earth or Yttrium and X = Si or Ge) display a rich variety of magnetic structures due to sharp changes in magnetic exchange interactions between neighbouring manganese atoms, resulting from changes in chemical pressure. Observed variants in the magnetic structure include ferromagnetic (*f*), collinear & non-collinear antiferromagnetic (*a/f*), mixed axial *f* + planar *a/f*, and even incommensurate *a/f* structures. This remarkable behaviour is symptomatic of subtle changes in interatomic bond lengths, differentiated at sub-picometre length scales. Transformation between magnetic variants is often accompanied by structural distortions due to magnetoelastic coupling. Further to this, we find that some pseudoternaries, in which one or more sites has mixed occupancy (e.g. La & Y mixed on the R site or Si & Ge mixed on the X site), simultaneously display two structural variants with different axial magnetic order (*f or a/f*). Such behaviour is most clearly seen in $PrMn_2Ge_{2-x}Si_x$ compounds where $x \approx 1$.

We report a neutron diffraction study on the $PrMn_2Ge_{2-x}Si_x$ system, through which we gain new insights into the magnetic and structural origins of the curious behaviour of these compounds. In certain regions of the phase diagram we clearly see phase separation (both structural and magnetic), which leads us to propose a two-phase structural model driven by changes in the Mn-Mn magnetic exchange energy, and related to variations in local strain propagated by the shared crystallographic sites. This interpretation brings into question whether a random substitution could produce such remarkable magnetoelastic phenomena or whether local site-specific atomic order is prevalent in the family of mixed 122 compounds.

T4

Temperature dependence of the spontaneous remagnetization in $Nd_{60}Fe_{30}Al_{10}$ and $Nd_{60}Fe_{20}Co_{10}Al_{10}$ bulk amorphous ferromagnets

S. J. Collocott

CSIRO Materials Science and Engineering, Lindfield, NSW, Australia 2070.

Time dependent behaviour of the magnetization, i.e. magnetic viscosity, in ferromagnetic materials is well known [1]. Less well known, and as a consequence little studied, is the phenomenon of spontaneous remagnetization. Spontaneous remagnetization is observed following dc demagnetization, where the magnetization is seen to increase monotonically with time [2]. Spontaneous remagnetization is largest in bulk amorphous ferromagnets, compared to related crystalline ferromagnetic materials under the same experimental conditions, making them well suited for studying time and temperature dependent behaviour.

Spontaneous remagnetizaion behaviour of the bulk amorphous ferromagnets $Nd_{60}Fe_{30}Al_{10}$ and $Nd_{60}Fe_{20}Co_{10}Al_{10}$ is investigated as a function of temperature from 50 K to 400 K. At all temperatures the spontaneous remagnetization, M_{spon}, follows the relationship $M_{spon} = S_{spon}\ln(t+t_0)$, where S_{spon} is a measure of the spontaneous remagnetization processes, t the time, and t_0 a reference time. For both alloys, in the temperature range 50 K to 290 K the variation of S_{spon} is roughly proportional with temperature, with the $Nd_{60}Fe_{30}Al_{10}$ alloy more closely approximating simple linear behaviour. Above 290 K, for both alloys, S_{spon} departs from simple linear behaviour, reaching a peak at around 300 K and 340 K for $Nd_{60}Fe_{30}Al_{10}$ and $Nd_{60}Fe_{20}Co_{10}Al_{10}$, respectively, and then decreases rapidly. This behaviour is similar to that observed for the magnetic viscosity coefficient, S, in a range of ferromagnetic materials [3].

[1] R. Street and S. D. Brown, J. Appl. Phys. **76**, 6386 (1994).

[2] S. J. Collocott and J. B. Dunlop. Proc. of the Twentieth International Workshop on Rare-Earth Magnets and Their Applications(REPM'08), edited by D. Niarchos (Admore, Athens, 2008), p. 45.

[3] S. J. Collocott. J. Appl. Phys. **107** 09A729 -3 (2010)

T5

Engineering Graphene Growth

Nikhil Medhekar,

Department of Materials Engineering, Monash University

For the last few years, graphene has been at the center of tremendous scientific attention in the field of condensed matter physics and chemistry. The explosion of interest in graphene is driven largely by its novel electrical, mechanical and thermal properties - the properties that can potentially lead to its application in the next-generation opto-electronic, spintronic and energy devices. While the scientific novelty of graphene has now been firmly established, the focus of the research has begun to shift into the engineering or technological domain. In particular, in order to achieve its true potential, we must be able to grow large and defect-free layers of graphene in a mass-scale and reproducible manner. In this talk, I will present an overview of the current state-of-the-art growth methods, highlighting challenges and opportunities in each.

T6

101 Uses for the Nitrogen-Vacancy Centre in Diamond

Neil B Manson

Laser Physics Centre, Research School of Physics and Engineering

Australian National University, Canberra, ACT, 0200

Shine green light on a diamond containing nitrogen-vacancy defects and it will emit red light. The green light pumps all the population into one spin state giving a spin temperature of micro Kevin at room temperature. The emission is then bright. Change the spin state for example with microwaves or magnetic field and the emission will become less bright.

The above simple property lead to there being many many applications for NV diamonds noting the observations can be at a single defect level. It is also significant that carbon is biocompatible. Details of some of the applications will be given.

T7

Hard-ball modeling of BCC to closest-packed transition in nanoscale shape memory alloy actuators

M.B. Cortie [a] and D.L. Cortie [b]

[a] *Institute for Nanoscale Technology, University ofTechnology Sydney, PO Box 123, Broadway, NSW2007, Australia.*

[b] *Department of Physics, University of Western Australia,* 35 *Stirling Highway, Crawley, Perth, Western Australia 6009*

The austenite-to-martensite transformation in shape memory alloys is associated with the transition from a high-temperature, body centred cubic structure, to a low-temperature closest-packed arrangement of atoms, where the low-temperature arrangement is in practice a heavily faulted version of face centered cubic or hexagonal close-packed structures. The increase in density causes an associated elastic strain during the transformation, which can be harnessed to drive an actuator.

Since the shape-memory effect is driven by changes in packing density, we considered that it would be instructive to simulate the process using a hard-ball atomistic model of the microstructure in which the Metropolis Monte Carlo scheme is used to drive the system to its state of lowest energy (and highest packing density). A Lennard-Jones type potential was used but the software is completely general and this interatomic potential can be replaced with any other. One of the issues in these types of simulations is that the computer processing requirements grow very rapidly with the number of spheres in the simulation. Here we employ a novel strategy to speed the simulation : we offload the calculation of sphere-to-sphere distance and neighbourly-ness to the DirectX graphics system often found on Windows machines. This highly optimized platform can handle the interactions between up to twenty thousand spheres, with at least an order of magnitude improvement in processing speed compared to code written in a conventional programming language.

The defect structure and strain in a shape-memory alloy cantilever is investigated using the new software. The simulation provides a realistic microstructure, with multiple domains, and a heavily faulted stacking sequence. These can be readily imaged and examined using 3D graphics software.

T8

Structural variety in brownmillerite-type materials

H. Krüger[a,b]

[a] *Research School of Chemistry, Australian National University, ACT, Australia.*

[b] *Institute of Mineralogy and Petrography, University of Innsbruck, Austria.*

Brownmillerite (Ca_2FeAlO_5) is one of the four major phases in Portland cement clinkers and plays an important role in the hydration process of cements. Furthermore, brownmillerites are extensively studied due to their magnetic and catalytic properties.

Brownmillerite-type structures ($A_2B_2O_5$) belong to the class of oxygen-deficient perovskites, where the vacancies are ordered in such a way that layers of tetrahedral chains are formed. Perovskite-like layers of corner-sharing [BO_6]-octahedra (O) alternate with sheets of [BO_4]-chains (T). The tetrahedral chains can adopt right- (R) or left-handed (L) configurations. With respect to different inter- and intra-layer ordering of R and L chains, a variety of structures exist. High-temperature phase transitions to commensurately and incommensurately modulated phases were found in the series $Ca_2(Fe_{1-x}Al_x)_2O_5$ [1].

The closely related *layered brownmillerites* ($A_4B_3O_9$) exhibit OTO brownmillerite blocks, which are connected by sheets of the halite structure type (similar to n=3 Ruddlesden-Popper phases) [2]. These layered structures show stacking faults as well as local ordering of the stacking sequences, according to commensurate and incommensurate structures. However, all possible structural variants of the *layered brownmillerites* can be described in one superspace group using the (3+1)-dimensional superspace approach.

The presentation will give an overview on structures and superstructures in brownmillerites and *layered brownmillerites*, including recent results.

H. Krüger, V. Kahlenberg, V. Petříček, F. Philipp and W. Wertl, *J. Solid State Chem.* **182** 1515 (2009).

N. Barrier, D. Pelloquin, N. Nguyen, M. Giot, F. Boure and B. Raveau, *Chem. Mater.* **17**, 6619 (2005).

T9

The structure of Yttria-Stabilised Zirconia: A combined medium energy photoemission and ab-initio investigation.

G. Cousland[a,b], L. Wong[b], M. Tayebjee[b], D. Yu[b], G. Triani[b], A. P.J. Stampfl[b,c], X. Cui[a], C. M. Stampfl[a], and A. Smith[d]

[a] *School of Physics, The University of Sydney, NSW 2006, Australia.*

[b] *Australian Nuclear Science and Technology Organisation, Lucas Heights, NSW 2234, Australia.*

[c] *School of Chemistry, The University of Sydney, NSW 2006, Australia.*

[d] *School of Physics, Monash University, Clayton, Victoria 3800, Australia.*

Cubic zirconia-based materials are candidates for use in the nuclear fuel cycle. There are three phases of ZrO2, a room temperature monoclinic phase and higher temperature tetragonal and cubic phases. The cubic phase of zirconia, in comparison to the other phases, exhibits a very low thermal conductivity, allowing the material to be potentially used in high temperature fission and fusion environments. Interestingly, the cubic-phase may be stabilised at room temperature through the addition of small quantities of other oxides for example, Y2O3, CaO and Ce2O3. Recent ab initio calculations for yttria-stablised zirconia (YSZ) predict the atomic geometry for various oxygen-vacancy containing structures [1]. In particular, a set of "rules" is used to establish a structure for 6.25 Mol % [1,2]. This model is extended to a yttria content of 9.375 Mol % and compared with a sample of 9.5 Mol % yttria.

Using this model, core-level shifts are estimated as changes in binding energy obtained from density-functional theory (DFT) calculations, due to the different chemical environments. The partial density-of-states of Y atoms differ depending upon whether there are oxygen vacancies at nearest-neighbour sites to the Zr atoms. Experimentally, a number of different core-levels and Auger-lines are acquired across the L-edges of Zr and Y. By measuring through the Y L-edge resonance, three distinct Zr environments and three distinct oxygen environments are observed in photoelectron peaks. The area under each peak is plotted against photon energy.

[1] D. Muñoz Ramo and A. L. Shluger, *J. Phys.: Conf. Ser.* **117**, 012022 (2008).

[2] A. Bogicevic, C. Wolverton, G. M. Crosbie, and E. B. Stechel, *Phys. Rev. B* **64**, 014106 (2001).

T10

Positron Annihilation Lifetime Spectra of Radiation Damaged, Natural Zircon Crystals

J. Roberts a, E. R. Vance b, J. Sullivan a, S. Buckman a, J. Davis b, P. Guagliardo c, M. Zhang d and I. Farnan d

a Centre for Antimatter-Matter Studies, Research School of Physical Sciences, Australian National University, Canberra, ACT, 2600, Australia

b Institute for Materials Engineering, ANSTO, Menai, NSW, 2234, *Australia*

c *Physics Dept University of Western Australia, Crawley, WA 6009, Australia*

d Dept of Earth Sciences, University of Cambridge, Cambridge, UK

Radiation damage in zircon is derived from radioactive decay of U and Th in solid solution over geological periods of time. It has been argued by Rios et al.[1] that at heavy alpha-doses, corresponding to about the half the dose for complete amorphism, small-angle X-ray scattering experiments provide evidence for the formation of nanovoids.

Here we have studied four natural zircons by positron annihilation lifetime studies, using both the ANU materials slow positron beamline and laboratory apparatus. Both methods show evidence of long lifetime components, although the agreement between the different methods is only qualitative. Zoning of radiation damage has been studied by scanning electron microscopy and the differences between the results using different methods are attributed to the different regions of samples interrogated by the positrons. Subsequent annealing of the samples at 700°C and then 1200°C has been carried out with beam based lifetime measurements occurring at each step.

[1] S. Rios and E. K. H. Salje, Density fluctuations in α-decay self-irradiated zircon, Appl. Phys. Lett., 84, 2061 (2004)

T11

Experimental study of diffusion and clustering in aluminium alloys

M.D.H. Lay[a], C.R. Hutchinson[a,b], T.J. Bastow[a] and A.J. Hill[a]

[a] *CSIRO Materials Science & Engineering, Clayton South VIC 3169, Australia.*

[b] *Department of Materials Engineering, Monash University, Clayton VIC 3800, Australia.*

High strength aluminium alloys remain important for the aerospace and automobile industries. The process which enables this strengthening to occur is based on the nucleation of nano-scale solute clusters or precipitates containing the alloying components (e.g. Si, Mg and Cu). The precipitation kinetics in aluminium alloys have yet to be fully understood, although it is known that there may be several stages of evolution with various stages of clustering and precipitation [1]. The details of the decomposition and the means to tailor routes and kinetics of precipitation are the subject of much current research. The dynamics of precipitation depends on solute diffusion and this is a process that is mediated by vacancies. The interactions between solutes and vacancies therefore strongly affect solute diffusion and subsequently precipitation. A binding energy can be defined which relates the free energy of vacancy formation in the vicinity of a solute atom to the free energy of formation in the matrix and this is a useful measure of the effects of solutes on vacancy diffusion.

We have studied the interaction between vacancies and solute atoms, in binary Al alloys, to calculate the vacancy solute binding energies through direct measurement of vacancy diffusion using positron annihilation lifetime spectroscopy.
By using solid-state nuclear magnetic resonance spectroscopy (NMR) we can also quantify the amount of solute clustering and the phase of the clusters within samples. These studies are also complemented by studies of solute clustering using X-ray absorption fine-structure spectroscopy (XAFS). A unique feature of XAFS, when compared to electron microscopy, NMR, and atom probe microscopy, is that XAFS requires little sample preparation and small amounts of material. This allows us to examine the effect of well-controlled, loading conditions (e.g. tension, compression and fatigue) on samples.

[1] A. Fontaine, P. Lagarde, A. Naudon, D. Raoux, and D. Spanjaard, *Philos. Mag. B.* **40**, 17 (1979).

T12

Neutrons and Li-Ion Batteries

N. Sharma[a] and V. K. Peterson[a]

[a]*The Bragg Institute, Australian Nuclear Science and Technology Organisation, Locked Bag 2001, Kirrawee DC NSW, Australia.*

Li-ion batteries are one of the most extensively studied energy storage devices in the world today. These batteries are found in mobile phones and laptop computers, but future applications may include electric vehicles and energy storage systems for smart electricity grids based on renewable intermittent power generation sources, promising to fundamentally change how we live. The in-depth understanding of the processes occurring in Li-ion batteries is crucial for further development of these technologies.

Neutron diffraction to study components within Li-ion batteries has distinct advantages. These include high sensitivity towards Li and a large penetration depth for bulk analysis of real-life Li-ion batteries. This talk will highlight recent results from *in-situ* [1] and *ex-situ* neutron diffraction studies of electrode materials in Li-ion batteries. In particular, the simultaneous tracking of lattice parameters of graphite anodes and $LiCoO_2$ cathodes in commercial Li-ion batteries, development of specialised batteries for *in-situ* experimentation, crystal-structure investigations of Li-insertion, and the elucidation of structure-property relationships of electrodes in Li-ion batteries.

This work is aimed at providing a real-time understanding of critical structural processes occurring at the electrodes and highlights the insights obtainable by marrying together neutron-diffraction with electrochemistry.

N. Sharma, V. K. Peterson, M. M. Elcombe, M. Avdeev, A. J. Studer, N. Blagojevic, R. Yusoff and N. Kamarulzaman, *J. Power Sources* **195**, 8258 (2010).

F1

Advanced resonant X-ray diffraction applied to the study of ordering phenomena in complex oxides

Annemieke Mulders
School of Physical, Environmental and Mathematical Sciences,
UNSW@ADFA, Canberra ACT 2600, Australia.

Competing interactions of spin and orbital moments, polar displacements and structural distortions lead to many interesting phenomena such as unconventional superconductivity, metal insulator transitions, colossal magnetoresistance and multiferroicity.
Resonant x-ray diffraction (RXD) is an invaluable technique to investigate these magnetic, orbital and structural properties. RXD intensities are much enhanced and probe the electronic properties of the virtually excited state directly. Besides magnetic and orbital order, it can observe higher order and magnetoelectric moments. These more exotic electronic properties may play a significant role in the development of novel advanced materials.

After an overview of the RXD technique and its achievements, our recent results on multiferroic materials will be presented. Multiferroics exhibit strong electric and magnetic polarizations simultaneously and they have the potential to dramatically increase data storage capacity and processing speeds. Competing theories of inherent electronic structure and ionic displacement have attempted to explain the coupling of the polarizations, but no experimental evidence currently exists to distinguish between the models.
We investigate hexaferrite $Ba_{0.8}Sr_{1.2}Zn_2Fe_{12}O_{22}$ which exhibits multiferroic behavior arising from frustrated spin order. The electric polarization appears with applied magnetic fields of about 0.5 Tesla. Our XRD study suggests that, besides the magnetic order, there is an additional order parameter in the multiferroic phase of hexaferrite below ~200 K.

F2

Cu_5SbO_6 – Synchrotron, Neutron Diffraction Studies and Magnetic Properties

T. Söhnel[a], E. Rey[a], C. Ling[b,c], M. Avdeev[c], B. Johannesson[d], K. Wallwork[d], R. Kremer[e], and M.-H. Whangbo[f]

[a] *Department of Chemistry, The University of Auckland, New Zealand.*
[b] *School of Chemistry, The University of Sydney, Sydney, Australia.*
[c] *Bragg Institute, Australian Nuclear Science and Technology Organisation, Menai, Australia.*
[d] *Australian Synchrotron, Clayton, Australia.*
[e] *Max Planck Institute for Solid State Research, Stuttgart, Germany.*
[f] *Department of Chemistry, North Carolina State University, USA.*

One very interesting compound in the system Cu/Sb/O is the mixed-valent Cu_5SbO_6 = $(Cu^{1+}(Cu^{2+}_{2/3}Sb^{5+}_{1/3})O_2)$ which is crystallising in the high temperature modification as a modified Delafossite structure type. Compounds like Delafossite, $CuFeO_2$, is one of the few groups of compounds showing the rare property of multiferroic behaviour. In Cu_5SbO_6 the magnetically active brucite-like CuO_2 layer is diluted in an ordered fashion with non-magnetic Sb^{5+}.

Cu_5SbO_6 also shows a phase transition, which exhibits a rather complicated behaviour. It depends on the temperature and the reaction conditions (reactants for preparation, pressure, open or closed system). High resolution Synchrotron and neutron powder diffraction measurements could clearly distinguish between the high temperature and the low temperature modification and reveal an ordering (HT-modification) / disordering (LT-modification) effect of the Sb^{5+} and Cu^{2+} ions in the brucite-like layers. The LT-modification can also be assigned to what had wrongly been described in the literature as $Cu_{4.5}SbO_5$.

XANES Cu-K edge measurements and NPD measurements should clarify a potential oxidation of the Cu^{1+} to Cu^{2+} and a connected additional inclusion of oxygen in the structure.

According to magnetic measurements and DFT calculations the magnetic structure in Cu_5SbO_6 can be described with a short range ferromagnetic-antiferromagnetic interaction model of the (Cu^{2+}) pairs in the $(Cu^{2+}_{2/3}Sb^{5+}_{1/3})O_2$ layers with a super-exchange via the non-magnetic Sb^{5+} atoms. The systematic replacement of the non-magnetic Sb^{5+} with magnetically active M^{5+} ions should change the magnetic properties dramatically and could lead to an long range ordering in the system. First results of Mn and Mo doping will also be presented.

F3

Comparison investigation for flux pinning of Titanium and Zirconium doped $Y_1B_2C_3O_{7-\delta}$ films prepared by TFA-MOD

Q. Li[a], D.Q. Shi[a], L. Wang[a], X.B. Zhu[b], S.X. Dou[a]

[a] *Institute for Superconducting and Electronic Materials, University of Wollongong, Northfields, Ave., Wollongong 2522, Australia.*

[b] *Key Laboratory of Materials Physics, Institute of Solid State Physics, Chinese Academy of Sciences, Heifei 230031, People's Republic of China.*

$Y_1B_2C_3O_{7-\delta}$(YBCO) is one of the most promising superconducting materials for practical applications since its related high critical temperature (T_c), high irreversibility field (H_{irr}), and high critical current (J_c). Recently, numerous researches have been carried out for inducing artificial pinning centers into YBCO matrix due to real superconducting products demand higher J_c. Second phase doping with chemical solution deposition (CSD) is one of the most property-effective and cost-efficient methods, especially for large-scale applications. In this work, Titanium (Ti) and Zirconium (Zr), which both locate in IVB group of elements periodic table, were introduced into YBCO film using trifluoroacetates metal organic deposition (TFA-MOD) route. Hexagonal $BaTiO_3$ (BTO) and cubic $BaZrO_3$ (BZO) second phase particles were respectively detected in Ti and Zr doped YBCO films which grew along highly c-axis orientation on $LaAlO_3$ substrate. Field-dependent J_c showed significant different on both films, as well as angle-dependent J_c. The results indicate the functional pinning centers in Ti and Zr doped YBCO are quite unlike although the physical and chemical properties of both doping elements are similar. The intrinsic structure properties of BTO and BZO are identified under TFA-MOD processing, which can lead to disparate pinning functions for enhancing J_c. The investigation shows not only a novel pinning controlling method, but also a promising dual-doping system.

F4

Diffuse scattering from PZN

R.E. Whitfield[a] and D.J. Goossens[ab]

[a] *Research School of Physics and Engineering, Australian National University, Canberra, 0200, Australia.*

[b] *Research School of Chemistry, Australian National University, Canberra, 0200, Australia.*

PZN ($PbZn_{1/3}Nb_{2/3}O_3$) is a relaxor ferroelectric with a perovskite unit cell and has important industrial applications because of it strong piezoelectric effect. While is has been well studied the exact cause of their strong piezoelectric effect is not well understood. Neutron and X-ray single crystal diffuse scattering has been collected from PZN at a range of temperatures. Diffuse scattering is the scattering from the short-range order in the crystal while Bragg scattering is from the average structure. It allow insight into the local-structure and disorder on a nano-scale in crystals. X-ray PDF data has also been collect which gives insight into the phase transitions that cannot be seen with the single crystal diffuse scattering due to the limited ability to collect a number of temperatures. PDF is a complementary technique to single crystal diffuse scattering which allows a more quantifiable approach to analysing the temperature dependence of the disorder in the crystal. The crystal is modeled to simulate the local structure of the crystal and to produce the short-range order that is seen in the diffuse scattering. The disorder is introduced into the crystal model using Monte Carlo simulations which show the structure forms planer polar domains associated with the Pb displacement from their average positions in the 110 directions along with the displacement correlation between the other atoms.

F5

Multilayered Water-Based Organic Photovoltaics

Andrew Stapleton[a], Ben Vaughan[a], Elisa Sesa[a], Bofei Xue[a.b], Kerry Burke[a,b], Xiaojing Zhou[a], Glen Bryant[a], Oliver Werzer[a], Warwick Belcher[a], Erica Wanless[a], Paul C. Dastoor[a]

[a] *Centre for Organic Electronics, University of Newcastle, Callaghan, NSW, Australia*.

[b] *CSIRO Energy Technology, Newcastle, NSW, Australia.*

Water-based polymer nanoparticles offer the prospect of a addressing two of the main challenges associated with printing large area organic photovoltaic (OPV) devices; namely how to control the nanoscale architecture of the active layer and eliminate the need for hazardous organic solvents during device production. However, to date, the efficiencies of nanoparticulate -based devices have been vastly inferior to that of the corresponding bulk-heterojunction structure. Here we present an approach for producing efficient OPV devices from polymer nanoparticulates through the fabrication of multilayered device architectures. We show that by controlling both morphology and inter-particle interactions it is now possible to build optimized OPV devices from aqueous dispersions of nanoparticles that are more efficient than the corresponding bulk heterojunction structure. This work offers the realistic prospect of the development of printable water-based photovoltaic materials.

F6

Study on the interfaces between organic and inorganic semiconductors

Ateeq-Ur- Rehman[1, 2], Hanjie Zhang[1], Qian Huiqin[1], Jin Dan[1],
Weidong Dou[1], Haiyang Li[1], Pimo He[1], Shining Bao[1]

[1]*Physics Department, Zhejiang University, Hangzhou 310027, People's Republic of China*
[2]*Physics Department, Forman Christian College University, Lahore-Pakistan*

The electronic structure of the FePc /Si (110) interface was studied by combined XPS and UPS measurements during the growth of organic molecules on substrate. At the coverage of 1.0 ML, the peaks relative to the features from the organic molecule are located at 2.56, 4.90, 7.90 and 10.88 eV below the Fermi level respectively, and shift to 2.73, 4.90, 7.74 and 10.52 eV when the coverage is 10 ML. With increasing the coverage, the cutoff of the HOMO shifts from 2.02 to 2.13 eV. During the deposition, C 1s orbital of pyrrole carbon linked to nitrogen shifts relative to Si2p by 0.3 eV which suggests that more electron charge transfer from this orbital into the substrate. After the electron charge transfers from the molecule to the substrate, the dipole layer is formed by the molecule's polarization on the Si substrate.

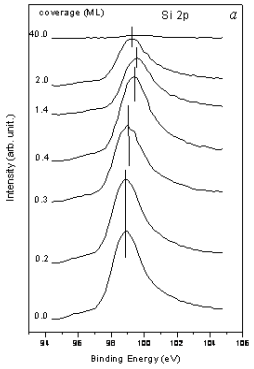

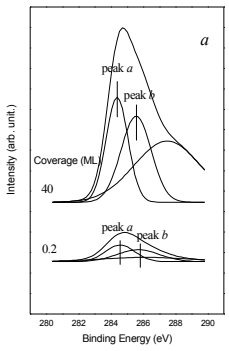

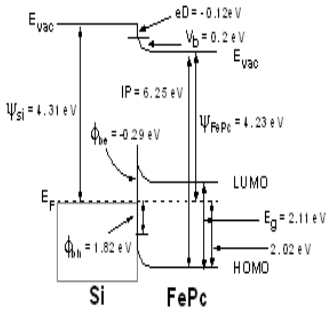

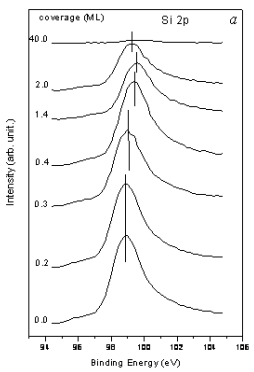

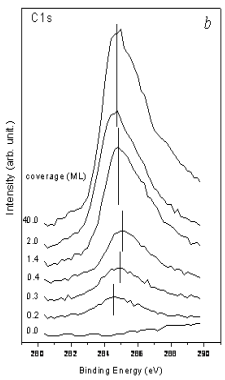

F7

Slow Photon Photocatalytic Enhancement in Titania Inverse Opal Photonic Crystals

V. Jovic[a], G.I.N Waterhouse and T. Soehnel[a]

[a] *Department of Chemistry, The University of Auckland, Auckland 1142, New Zealand.*

Titania (TiO_2) inverse opal thin films and powders possessing photonic band gap (PBG) positions in the UV and visible regions of the electromagnetic spectrum were successfully fabricated using the colloidal crystal template approach. Colloidal crystal templates with varying sphere diameters were prepared by the self-assembly of monodisperse poly(methyl methacrylate) (PMMA) colloidal suspensions into ordered FCC lattice arrays. After drying the colloidal crystal templates were infiltrated by a TiO_2 sol-gel precursor and the resulting structures were calcined at 450°C to remove the PMMA colloidal crystal templates. The TiO_2 inverse opals obtained were characterised by SEM, XRD, NEXAFS, BET surface area and BJH pore size distribution methods. Results showed an FCC array of air spheres in a high surface area nanocrystalline anatase TiO_2 matrix. UV-Vis transmittance measurements showed that the optical properties of the PMMA colloidal crystal templates and TiO_2 inverse opals photonic crystals followed the modified Braggs law equation in terms of PBG position as a function of lattice spacing, D, angle of interacting light, θ, and the average refractive index of the structure, n_{avg}.[1] The photocatalytic activities of the TiO_2 inverse opal photonic crystal powders were tested by observing the gas phase photodecomposition of ethanol. Results showed that the slow photon [2] effect coupled with the electronic band gap of TiO_2 has given an enhanced photocatalytic rate over a commercially used TiO_2 photocatalysts.

[1] R. C Schroden, M. Al-Daous, C.F. Blanford, A. Stein, A. *Chem. Mater*, **14**, 3305-3315 (2002)

[2] J. I. L, Chen, G. von Freymann, S.Y. Choi, V. Kitaev, G.A. Ozin, *J. Mater. Chem,* **18**, 369-373 (2008)

WW2011 ABSTRACTS FOR POSTER SESSIONS

Abstracts for poster sessions are listed in first author alphabetical order.

WP1

Possible Pd-vacancy pairing in germanium: Dependence on doping and orientation

Adurafimihan A. Abiona[a,*] William.J. Kemp[a], Aidan P. Byrne[b],
Mark Ridgway[b] and Heiko Timmers[a]
[a]*School of PEMS, The University of New South Wales, Canberra, Australia*
[b]*RSPS, Australian National University, Canberra, Australia*
[*]*On leave from Centre for Energy Research and Development, OAU, Ile-Ife, Nigeria*

Time Differential Perturbed Angular Correlation (TDPAC) measurements were performed in intrinsic germanium with the ^{100}Pd /^{100}Rh probe which was produced via ^{92}Zr(^{12}C, 4n) ^{100}Pd and recoil-implanted. As reported in previous work [1], a modulation pattern in the ratio function $_{100}$Pd/$_{100}$Rh probe in intrinsic germanium is observed with a quadrupole interaction frequency of 8.3(2) Mrad/s. The pattern is most pronounced after annealing at 500 °C and disappears after annealing at 700 °C. Instead strong damping of the ratio function is observed. The pattern may be caused, similar to what has been observed for highly doped n-type silicon, by the pairing of the Pd-atom with a vacancy (as shown Fig.1) located in the <111> direction as nearest-neigbour [2]. The disappearance of the pattern would indicate the dissociation of this pair. Pair formation and dissociation may be relevant to palladium-induced-crystallization processing of germanium.

This work focuses on the verification that the vacancy is located in the <111> direction with TDPAC measurements for different sample orientations. Furthermore, the effect has been searched for in germanium samples with different p-type and n-type doping concentrations of Ga, In and As, respectively.

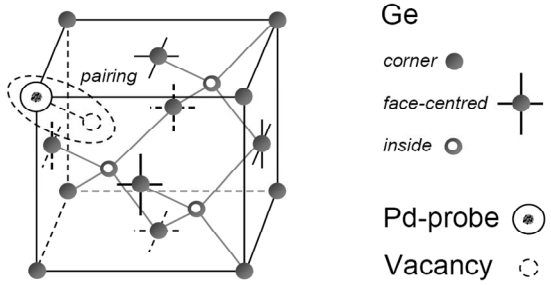

Figure 1: Illustration of the possible Pd-Vacancy defect complex in intrinsic germanium.

[1] H. Timmers, W. Kemp, A. P. Byrne, M.C. Ridgway, R. Vianden, P. Kessler, M. Steffens, *Hyperfine Interactions*. DOI: 10.1007/s10751-010-0206-3 (2010).

[2] R. Dogra, A.P. Byrne, M.C. Ridgway, *Journal of Electronic Materials*. **38**, 5 (2009).

WP2

Coherence properties of rare earth ion doped thin films

J.G. Bartholomew[a], S. Marzban[a], M.J. Sellars[a] and R.-P. Wang[a]

[a] *Laser Physics Centre, Australian National University, ACT 2600, Australia*

With the recent demonstration of a highly efficient and low noise quantum memory for light in a rare earth ion doped crystal[1], research now focuses on how to realise a practical device for quantum communication. One area of interest is the construction of rare earth ion doped crystalline waveguides[2]. Among the advantages of such structures is the ability to apply very strong electric fields which would enable the current bandwidth of the memory to be increased significantly.

Through the use of pulsed laser deposition, single crystals have been grown epitaxially onto compatible substrates. Materials including rare earth ion doped Y_2O_3, $YAlO_3$ and YAG can be grown to a subwavelength thickness. However, the critical issue is determining the growth conditions to preserve the long optical coherence times measured in bulk samples at liquid helium temperatures.

The characterisation of the optical properties of the rare earth ions in the crystalline films can be performed via several techniques including inhomogeneous broadening spectra, holeburning spectroscopy and photon counting-photon echo (PCPE) studies. Of these the last is the most critical technique for determining whether such films are suitable for waveguide quantum memories. The PCPE technique allows coherent signals to be detected from as few as a thousand optically active ions with minimum signal detection on the order of 30 photons per second. Thus, it is feasible to study the performance of the optical centres in films as thin as 10s of nanometers.

[1] M. P. Hedges, J. J. Longdell, Y. Li, and M. J. Sellars, *Nature* **465**, 1052-1056 (2010).

[2] N. Sinclair, E. Saglamyurek, M. George, *et al*., *Journal of Luminescence,* **130**(9):1586-1593 (2010).

WP3

Ab initio determination of the structure of the ferroelectric phase of $SrTi^{18}O_3$

M Bartkowiak[1,2], G J Kearley[2], M Yethiraj[2] and A M Mulders[1]
[1]*School of Physical, Environmental and Mathematical Sciences, UNSW@ADFA, Canberra ACT 2600, Australia*
[2]*Bragg Institute, ANSTO, Lucas Heights NSW 2234, Australia*

.

Strontium titanate ($SrTi^{18}O_3$) is known to display a quantum paraelectric behavior. Its dielectric constant saturates at low temperatures and does not increase with cooling due to quantum fluctuations present in the system. Only in 1999 Itoh *et al* [1] discovered that substituting regular ^{16}O with the ^{18}O isotope stabilizes the system and allows a transition into a ferroelectric phase below 23 K.

The mechanism of the transition and the structure of the new phase have not been conclusively determined by experiment. The new phase displays ferroelectric properties and there are new peaks present in the Raman spectrum. However, diffraction experiments indicate that the structural distortion accompanying the transition is minimal, while Raman and NMR measurements provide evidence for both the order-disorder mechanism and the displacive mechanism to be an applicable explanation of the transition.

We applied density functional theory calculations and lattice dynamics analysis to show that the paraelectric tetragonal phase of the regular $SrTiO_3$ is inherently unstable. By distorting the structure along the direction of the soft mode present at the centre of the Brillouin zone we obtained an orthorhombic, ferroelectric structure of $SrTiO_3$ which is energetically favourable over the paraelectric one. Lattice dynamics calculations show that our new structure is stable and the frequencies of the phonon modes present in it are in good agreement with the experimental values published so far.[2]

[1] M. Itoh, R. Wang, Y. Inaguma, T. Yamaguchi, Y. Shan and T. Nakamura, Physical Review Letters 82, 3540 (1999)
[2] M. Bartkowiak, G. J. Kearley, M. Yethiraj and A. M. Mulders, submitted to Phys. Rev. B. (2010)

WP4

Precipitate growth in a mechanically stressed (deformed) Al(Cu,Li,Mg,Ag) alloy observed by ^{7}Li, ^{27}Al and ^{63}Cu NMR and XRD

T.J.Bastow [1] , C.R.Hutchinson [2] A Desachamps [3] and A.J.Hill [1]

[1] *CSIRO Materials Science and Engineering, Clayton, Victoria 3168*

[2] *Dept. of Materials Engineering, Monash University, Clayton, Victoria 3800,*

3 SIMAP, INPGrenoble-CNRS_UJF, BP 75, 38402 St Matin d'Heres Cedex, France

Al-Cu-Li alloys are lightweight industrially important structural materials consisting typically of Al with approximately three weight percent each of Cu and Li. They present difficulties in manufacture due to Li volatility during formation from the melt. Their virtue lies in their high strength allied with relatively low density. Their mechanical strength derives from Al, Cu and Li-containing intermetallic precipitates which are formed by initial solution treatment followed by a water quench and suitable heat treatment.

A number of distinct binary and ternary phases Al-Cu-Li alloys have been identified in Al-Cu-Li alloys; viz Al_3Li (δ′), AlLi (β), Guinier-Preston zones (GP), Al_2Cu (θ′), Al_2CuLi (T_1), Al_6CuLi_3 (T_2) and Al_7Cu_4Li (T_B). The dominant precipitate forming in Al-Cu-Li alloys after heat treatment around 200^{o}C, is generally agreed by metallurgists to be T_1 phase, hexagonal Al_2CuMg. The concentration of T_1–phase is reported to be enhanced by mechanical deformation and the presence of trace quantities of Ag .

We report an NMR/XRD experiment with the alloy Al(1.4 Cu, 3.9Li, 0.6Mg, 0.08Ag, 0.03Zr), with concentrations in at%,, where deformation produced a dominant precipitate which was *not* T_1 but the strictly cubic phase T_B (proposed formula Al_7Cu_4Li) which has a strong structural and chemical similarities to Al_2Cu (θ′). The NMR probes used were the naturally abundant stable isotopes of the three main constituent elements, viz ^{7}Li, ^{27}Al and ^{63}Cu. The XRD characterisations for these very dilute precipitate systems were made at the Australian Synchrotron powder diffraction beamline. It is emphasised that a great potential benefit results from using highly collimated, high intensity synchrotron beams for XRD, in conjunction with solid state NMR, to provide a *bulk* quantification of precipitate content of these lightweight alloys. This overall aspect is lacking from TEM and atom probe characterizations.

Acknowledgement

Part of this research was undertaken on the Powder Diffraction beamline at the Australian Synchrotron, Victoria, Australia

WP5

Studying multiferroic $BiFeO_3$ and ferromagnetic $La_{0.67}Sr_{0.33}MnO_3$ tunnel junctions with Raman spectroscopy and neutron scattering techniques

J. Bertinshaw[a,b], T. Saerbeck[c], A. Nelson[b], M. James[b], V. Nagarajan[d], F.Klose[b], C. Ulrich[a,b]

[a] *School of Physics, University of NSW, NSW, Australia.*

[b] *Bragg Institute, ANSTO, NSW, Australia*

[c] *School of Physics, University of Western Australia*

[d] *School of Materials Science and Engineering, University of NSW, NSW, Australia.*

Bismuth Ferrite ($BiFeO_3$ or BFO) is a prominent multiferroic material candidate for industrial implementation as it is among one of the rare cases where ferroelectric polarisation and magnetic order coexist at room temperature [1]. We have investigated its potential in functional thin film heterostructures, where it is possible the interplay between FE and FM at the interface between layers can enable controllable magnetoelectric coupling, allowing for the control of the magnetic polarisation through applied electric fields and vise-versa [2].

Epitaxial (001) $BiFeO_3$ / $La_{0.67}Sr_{0.33}MnO_3$ (LSMO) multiferroic tunnel junctions have been grown by pulsed laser deposition at the University of NSW [3]. These trilayer systems layer: 40nm of LSMO, 10nm of BFO, and 40nm of LSMO on a $SrTiO_3$ substrate, with a RMS roughness of not more than one unit cell. We have found initial experimental evidence of a correlation between the spin polarisation of the FM LSMO layers and the FE polarisation of the $BiFeO_3$ layer through flips in the domain structure through a number of electrical resistance based experimental techniques [3].

We plan to combine results from Raman spectroscopy conducted at the UNSW with polarised neutron reflectometry on PLATYPUS and inelastic neutron scattering on TAIPAN at the Bragg Institute, ANSTO to perform a detailed analysis of: the magnetisation reversal process in the LSMO contact layers, the interplay (exchange bias) between the BFO AFM and LSMO FM parameters, the magnetic depth profile of the heterostructure, in particular the interface regions, and the effect of switching the electric polarisation of the $BiFeO_3$ layer on the domain wall structure, and therefore on the magnetic structure of the entire thin film system.

[1] Ramesh and Spaldin. *Nature Materials* **6**, 21 (2007)

[2] Tsymbal and Kohlstedt. *Science* **313**, 181 (2006)

[3] Hambe et al. *Advanced Functional Materials* **20**, 2436 (2010)

WP6

Identification of Fe^{3+} Site Coordinations in NAu-2 Nontronite

J.D. Cashion[a], W.P. Gates[b], T.L. Greaves[a,†] and O. Dorjkhaidav[a,#]

[a] *School of Physics, Monash University, Melbourne, VIC 3800, Australia.*

[b] *Department of Civil Engineering, Monash University, Melbourne, VIC 3800, Australia.*

Many clay minerals, such as the smectites, have mixed cations in their octahedral and tetrahedral sheets. In the tetrahedral sheets, these are typically Si^{4+} with Al^{3+} and possibly Fe^{3+}, while in the octahedral sheets, they are typically Al^{3+}, with Fe^{3+}, Mg^{2+} and possibly Fe^{2+}. The arrangement of these cations has a strong effect on the physical and chemical properties and hence its use, e.g. as a drilling mud or an impervious layer. The determination of the true cation distribution, rather than the average distribution, is very difficult.

Mössbauer spectroscopy has been a common technique used in this determination, but the resolution is limited and there have been disputes in the literature as to whether the two most common doublets should be assigned to *cis*- and *trans*-OH^- arrangements about the Fe^{3+} ion, or whether they are due to different, but unspecified, cation neighbour arrangements. We have recently shown [1] that the effect of different nearest neighbour cation configurations is larger than the *cis*-*trans* effect and have been able to correlate Mg^{2+} as producing the largest splittings. Furthermore, a study of the NAu-1 nontronite [2] enabled us to assign its two main subspectra to three specific coordinations of its three octahedral and eight tetrahedral neighbours. The present study of the related NAu-2 nontronite, which has a different composition, confirms these assignments. Furthermore, this nontronite has a significant proportion of its Fe^{3+} as interlayer cations and these produce a doublet with a wider quadrupole splitting than the structural ions, increasing our understanding of the systematics of correlating Mössbauer spectra with crystallographic configurations in these materials.

† Present address: CSIRO Molecular Health Technologies, Clayton, Vic 3169.

Present address: Dept. of Safeguards, I.A.E.A., Vienna, Austria.

[1] J.D. Cashion, W.P. Gates and A. Thomson, *Clay Miner.*, **43,** 83 (2008).

[2] J.D. Cashion, W.P. Gates and G. M. Riley, *J. Phys.: Conf. Series*, **217**, 012065 (2010).

WP7

Fermi Arc – Hole Pocket Dichotomy: Effect of Spin Fluctuation in Underdoped Cuprates

W. Chen and O. P. Sushkov

School of Physics, University of New South Wales, Sydney 2052, Australia.

We develop a generalized self-consistent Born approximation to study the effect of spin fluctuations at finite doping. The approach incorporates both antiferromagnetic ordering and spin spiral ordering in the ground state. We find that the electron spectral function at the chemical potential is highly anisotropic, which clearly resembles the Fermi arc feature observed in angle resolved photoemission in underdoped cuprates. On the other hand, our approach contains small hole pockets, so it is fully consistent with recently observed magnetic quantum oscillations.

WP8

Continuous-wave terahertz spectroscopy as a non-contact, non-destructive method for characterising semiconductors

E. Constable and R. A. Lewis

Institute for Superconducting and Electronic Materials, University of Wollongong, Wollongong NSW 2500, Australia.

Using the technique of terahertz photomixing, a continuous-wave terahertz source is adapted to characterize semiconductors in the range from 0.05 to 1.0 THz. By directly analysing the interference pattern of the transmission through semiconductor wafers using Fabry-Perot theory, information regarding the refractive index, carrier concentration and conductivity are obtained without physically contacting the sample. Materials studied include high-resistivity Si and ZnTe. The continuous-wave technique enables measurements to be made at much lower frequencies than those achievable with traditional fourier-transform spectroscopy or pulsed-wave time-domain terahertz techniques.

[1] K. Sakai, *Terahertz Optoelectronics*, Springer (2004).

[2] T.-I. Jeon, *Characterization of doped silicon from 0.1 to 2.5 THz using multiple reflection,* Journal of Optical Society of Korea, Vol.3 No 1, 10-14 (1999).

WP9

Pyrochlore-Fluorite Transition in $Y_2Sn_{2-x}Zr_xO_7$ - Implications for stability.

M. de los Reyes[a], K.R. Whittle[a], M. Mitchell[b], S.E. Ashbrook[b] and G.R Lumpkin[a]

[a] *Institute of Materials Engineering, ANSTO, Locked Bag 2001, Kirrawee DC, NSW, 2232, Australia*

[b] *School of Chemistry, University of St Andrews, St Andrews, Fife, UK*

The pyrochlore-fluorite transition is an important factor in determining how materials behave under conditions of irradiation, whether it be as a waste form or as a nuclear material, e.g. ODS additive. Yttrium based materials are often added as oxides to metallic systems, e.g. oxide dispersion strengthened (ODS) steels, which have a wide range of applications. As part of a large programme of research investigating and developing materials which show a high degree of radiation damage resistance, materials based on $Y_2Sn_{2-x}Zr_xO_7$ have been studied. The materials have been examined to determine the order-disorder transition (pyrochlore-fluorite), and how this effects the radiation damage resistance, particularly as both end members have previously been shown to be resistant to damage/amorphisation. Results are presented from diffraction and spectroscopic studies showing the degree of order/disorder within the system.

WP10

Mixed Spin-1 and Spin-3/2 Ising System with Two Alternative Layers of a Honeycomb Lattice within the Effective-Field Theory*

B. Deviren[a], S. Akbudak[b] and M. Keskin[c]

[a] *Department of Physics, Nevsehir University, 50300 Nevşehir, Turkey.*

[b] *Department of Physics, Adıyaman University,02040 Adıyaman, Turkey.*

[c] *Department of Physics, Erciyes University, 38039 Kayseri, Turkey.*

The two-sublattice mixed-spin Ising systems have been studied both experimentally and theoretically due to reason that these systems mainly related to the potential technological applications in the area of thermomagnetic recording [1]. Moreover, the mixed-spin Ising systems have less transitional symmetry than their single spin counterparts; hence exhibit many new phenomena that cannot be observed in the single-spin Ising systems, and the study of these systems can be relevant for understanding of bimetallic molecular systems based magnetic materials [2]. One of the well known mixed-spin systems is the mixed spin-1 and spin-3/2 Ising system [3]. In this work, an effective-field theory with correlations is developed for a mixed spin-1 and spin-3/2 Ising system with two alternative layers of a honeycomb lattice. Spin-1 atoms and spin-3/2 atoms are distributed in alternative layers of a honeycomb lattice. We consider that the nearest-neighbor spins of each layer are coupled ferromagnetically and the interaction between the vertically aligned spins and adjacent spins are coupled either ferromagnetically or antiferromagnetically depending on the sign of the bilinear exchange interactions. We investigate the temperature dependence of the total magnetization to find the compensation points and to determine the type of compensation behavior. We present the phase diagrams in different planes in the absence of the magnetic field, and the phase diagrams contain the paramagnetic, nonmagnetic and ferrimagnetic phases. The system also presents a tricritical behavior besides multicritical point (A), isolated critical point (C) and double critical end point (B) depending on the interaction parameters.

[1] M. Mansuripur, *J. Appl. Phys.* **61**, 1580 (1987).

[2] O. Kahn, in: E. Coronado, et al., (Eds.), *From Molecular Assemblies to the Devices*, (Kluwer Academic Publishers, Dordrecht, 1996).

[3] M. Keskin, E. Kantar, and O. Canko, *Phys. Rev. E* **77**, 051130 (2008).

---

* The work was supported by Erciyes University Research Fund, Grand No: FBY-10-3011.

WP11

Condensed Matter and Materials Trivia

J.B. Dunlop[a], T.R. Finlayson[b] and P. Gwan[c]

[a] *Davidson, New South Wales 2085, Australia.*

[b] *School of Physics, University of Melbourne, Victoria 3010, Australia.*

[c] *10 Silver Birch Close, Caves Beach, New South Wales 2281, Australia.*

The responses for numerous groups of attendees at the A&NZIP Annual Condensed Matter and Materials Meeting (the Wagga Meeting) to questions on subjects covering Current Events, Science, History, Geography, Sport, Music, Films and Absolute Trivia, have been analyzed using a rigorous statistical treatment. The groups have included a large cross section of persons from most of the States and Territories of Australia, New Zealand and several overseas countries. The data illustrate that such groups share a broad range of expertise for matters of trivia, with no particular bias towards questions concerned with the special subject of the Meeting itself. In addition, there appears to be little evidence for the retention of knowledge of Trivial Issues from one year to the next, on the parts of particular groups of attendees at the Meeting.

The data will be presented where appropriate in graphical and/or tabular form, with due attention to a proper statistical analysis of the results, providing sufficient confidence in the outcomes for the future of Wagga Trivia for all participants at this and all subsequent Wagga Meetings.

Several generations of “Wagga-ites” are acknowledged for the provision of the original data on which this research has been based.

WP12

Non-stoichiometric Mn Doping in Olivine Lithium Iron Phosphate: Structure and Electrochemical Properties

Chuanqi Feng [a], Hua Li [a], Guodong Du [b], Zaiping Guo [b]*, Neeraj Sharma [c]*, Vanessa K. Peterson [c], and Huakun Liu [b]

[a] *Key Laboratory for Synthesis and Applications of Organic Functional Molecules Hubei University, Wuhan 430062, (Peoples Republic of China)*

[b] *Institute for Superconducting & Electronic Materials, University of Wollongong, NSW 2522 (Australia) E-mail: (zguo@uow.edu.au)*

[c] *The Bragg Institute, Australian Nuclear Science and Technology Organization Locked Bag 2001, Kirrawee DC NSW 2232 (Australia) E-mail: (neeraj.sharma@ansto.gov.au)*

$LiFePO_4$ and $[Li_{0.918(10)}Fe_{0.01}][Fe_{0.99}Mn_{0.01}]PO_4$ or 1% Mn-doped $LiFePO_4$ were synthesized by the one-step rheological phase reaction method using inexpensive $FePO_4$ as the main raw material. Synchrotron X-ray diffraction, neutron powder diffraction, and transmission electron microscopy were used to characterize $LiFePO_4$ and Mn-doped $LiFePO_4$. Particle sizes were found to be distributed in the range of 0.5 to 1 μm and the carbon-content in the as-prepared samples was around 2 wt%. Rietveld analysis suggests 1 % Mn-doping replaces 1 % Fe from the Fe (*M*2) site and places this fraction of Fe on the Li (*M*1) site. The first process on the *M*2 site is isovalent doping (Mn^{2+} for Fe^{2+}), while the second process on *M*2 is supervalent doping (Fe^{2+} for Li^{+}). The second process requires that Li vacancies exist for charge balance and our simultaneous refinements against neutron and synchrotron X-ray diffraction data indicate an amount of Li vacancies consistent with this requirement. This doping regime agrees with the observed enhancement of the electrochemical properties of the Mn-doped $LiFePO_4$ compared to the undoped $LiFePO_4$. The Mn-doped $LiFePO_4$ cathodes exhibit higher capacity and better cycling performance than the pure $LiFePO_4$.

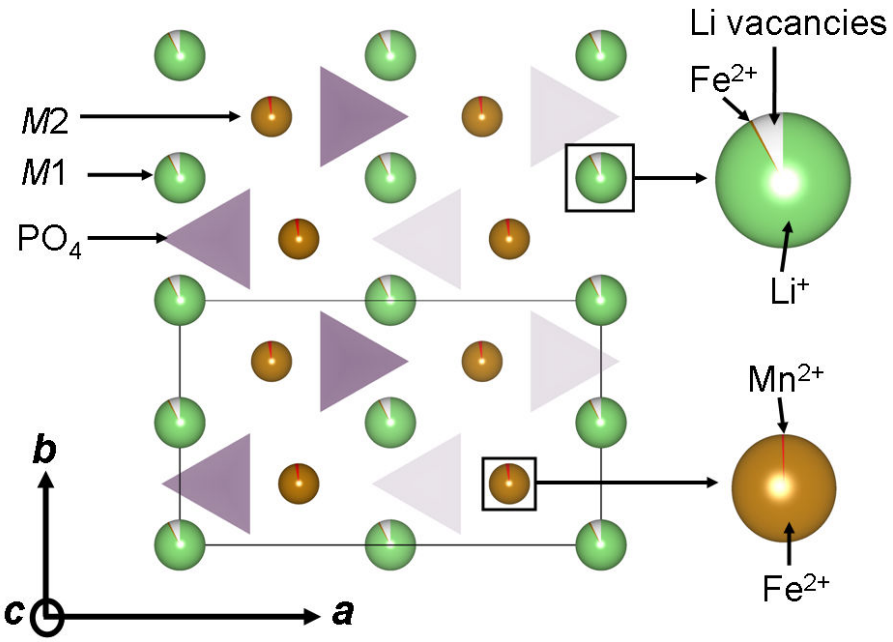

WP13

Anomalous Precursive Behaviour for the Martensitic Material $Ni_{0.625}Al_{0.375}$

T.R. Finlayson[a], S. Danilkin[b], A.J. Studer[b] and R.E. Whitfield[c]

[a] *School of Physics, University of Melbourne, Victoria 3010, Australia.*

[b] *Bragg Institute, ANSTO, Locked Bag 2001, Kirrawee DC, New South Wales 2232, Australia.*

[c] *Research School of Physics and Engineering, Australian National University, Canberra 0200, Australia.*

Ni_xAl_{1-x} alloys for $0.615 < x < 0.64$ undergo a martensitic transformation upon cooling from a CsCl-type structure to a pseudo-orthorhombic structure [1]. The transformation temperature is extremely composition dependent [2] and for $Ni_{0.625}Al_{0.375}$ is ~ 80 K [1]. In previous research using an approximate cube of single crystal having $x = 0.625$ [3], significant strain anisotropy was detected above 80 K. It was suggested that this anomalous strain anisotropy indicated the presence of a martensite precursor within the cubic "parent" phase.

The aim of the current research project is to investigate the precursive structural behaviour in the above $Ni_{0.625}Al_{0.375}$ single crystal using both elastic and inelastic neutron scattering. Results from initial experiments at both the Wombat and Taipan instruments at the Opal Research Reactor will be presented and discussed in relation to previously published strain anisotropy data determined using variable temperature, capacitance dilatometry [3].

Access to the Wombat and Taipan instruments through the ANSTO Bragg Institute User Programme is acknowledged as is the financial assistance from the Australian Institute for Nuclear Science and Engineering (AINSE) for travel and accommodation to enable TRF to undertake such experiments.

[1] S.M. Shapiro, B.X. Yang, G. Shirane, Y. Noda and L.E. Tanner, *Phys. Rev. Lett.* **62**, 1928 (1989).

[2] S. Chakravorty and C.M. Wayman, *Metall. Trans. A* **7**, 555 (1976).

[3] M. Liu, T.R. Finlayson, T.F. Smith and L.E. Tanner, *Mater. Sci. & Eng.* **A157**, 225 (1992).

WP14

Reliable shape information on prosthesis wear debris particles from atomic force microscopy

L. G. Gladkis [1,2], H. Timmers [1], Jennifer M. Scarvell [2], Paul N. Smith [2]

[1] School of Physical, Environmental and Mathematical Sciences,

University of New South Wales at ADFA, Canberra, ACT 2600

[2] Trauma and Orthopaedic Research Unit, The Canberra Hospital,

PO BOX 11, Woden, ACT 2606

Atomic force microscopy (AFM) is used to characterize in detail UHMWPE wear debris from a LCS knee prosthesis actuated with a constant load actuator. Fractionation of debris particles according to size was achieved with a new filtration protocol, developed by the authors. The size and shape of debris particles is quantified in all three spatial dimensions. Artificially limiting the analysis to the two-dimensional projections of the particles onto the substrate plane, it has been found that equivalent shape ratio (ESR) plotted as a function of equivalent circle diameter (ECD) follows a trend observed before. Inclusion of the third, vertical spatial dimension of particle height shows that such two-dimensional analysis, as it is often based on SEM images, can greatly misrepresent the actual particle shape. The three-dimensional AFM information indicates that for the prosthesis and the conditions studied here (water as lubricant, constant load actuator) debris particles tend to be deformed independent of their volumetric size.

A realistic wear simulation using a Prosim knee simulator was performed, particle debris created with this method was also analyzed. Results from both simulations will be compared.

WP15

A Frustrated 3D Antiferromagnet: Stacked J1 – J2 Layers

C.J. Hamer [a], Onofre Rojas [a,b] and J. Oitmaa [a]

[a] *School of Physics,The University of New South Wales, Sydney NSW 2052, Australia.*

[b] *Departamento de Ciencias Exatas, Universidade Federal de Lavras, Lavras, MG, Brazil.*

The study of frustrated quantum antiferromagnets remains an active field. A much studied model is the spin ½ square lattice with nearest and next-nearest neighbour interactions of strengths J_1 and J_2 (the 'J_1-J_2 model') [1]. This system has magnetically ordered ground states for both small and large J_2, with a magnetically disordered 'spin liquid' phase in the intermediate region $0.4 \leq J_2/J_1 \leq 0.6$. It has recently been argued [2] that the J1-J2 model provides a good description of the layered materials $LiVOSiO_4$ and $LiVOGeO_4$. These materials have $J_2/J_1 >> 1$, and are in the so-called 'columnar' phase.

Electronic structure calculations suggest that the coupling between planes is by no means negligible. For this reason, and for also purely theoretical reasons, we have studies a 3D system of J1-J2 layers, coupled by a nearest neighbour non-frustrating exchange J_3. We use series expansion methods to compute ground-state energies and magnetization as well as magnon spectra. The series results are also compared with 1st order spin wave calculations.

We find that interplane coupling J3 reduces the extent of the spin liquid phase, and that it vanishes completely for J3/J1 ~ 0.15, beyond which there is a direct transition between Neel and columnar ground states. In the 3D case the magnetically ordered phases will also persist to finite temperatures.

[1] O.P. Sushkov et al., Phys.Rev B**63**, 104420 (2001),J. Sirker et al., *ibid.***73**,184420 (2006).

[2] H. Rosner et al., Phys.Rev.Lett. **88**, 186405 (2002).

WP16

An ^{57}Fe-Mössbauer study of the magnetic phase diagram for $Nb_{1-x}Hf_xFe_2$

S.J. Harker[a], H. Okimoto[b], G.A. Stewart[a], K. Nishimura[b] and W.D. Hutchison[a]

[a] *School of Physical, Environmental & Mathematical Sciences, University of New South Wales, Australian Defence Force Academy, Canberra, ACT 2600, Australia.*

[b]*Graduate School of Science and Engineering, Toyama University, Toyama 930-8555, Japan.*

The intermetallic series $Nb_{1-x}Hf_xFe_2$ ($0 < x < 0.8$) forms with the hexagonal C14 Laves phase structure and exhibits a range of magnetic properties that are not yet fully understood. Stoichiometric $NbFe_2$ is a weak itinerant antiferromagnet with a Néel temperature of $T_N \approx 18$ K [1]. In its unannealed form, $HfFe_2$ forms with a minor C14 phase component (the preferred phase is cubic C15) that orders ferromagnetically at $T_C \approx 427$ K [2,3]. With increasing Hf concentration, the magnetic ordering temperature increases fairly smoothly between these two end values. However, the nature of the ordering varies between ferrimagnetic ($x = 0.2$, 0.3) and antiferromagnetic ($x = 0.4 – 0.7$) behaviour and it is difficult to arrive at precise ordering temperatures from the magnetization measurements recorded so far. $Nb_{0.2}Hf_{0.8}Fe_2$ is certainly ferromagnetic and there is a remarkable change in magnetic character between $x = 0.7$ and 0.8. There is also a low temperature region of spin glass-like behaviour ($x > 0.5$).

In this work, ^{57}Fe-Mössbauer spectroscopy is used to monitor the temperature dependence of the magnetic hyperfine fields acting at the 2a- and 6h- Fe sites and to determine the relevant magnetic ordering temperatures as a function of Hf concentration.

[1] Y. Yamada, H. Nakamura, Y. Kitaoka, K. Asayama, K. Koga, A. Sakata and T. Murakami, *J. Phys. Soc. Japan* **59**, 2967 (1990)

[2] K. Ikeda, *Z. Metallkde.* **68**, 195 (1977).

[3] J. Belosevic-Cavor, B. Cekic, N. Novakovic, N. Ivanovic and M. Manasijevic, *Mat. Sci. Forum*, **453-454**, 89-92 (2004)

WP17

Magnetic and structural properties of some compounds in the *MM*'PS3 family.

B. Hillman[a], D. James[a], J. Dong[b], W.D. Hutchison[c], D.J. Goossens[ab]

[a] *Research School of Chemistry, Australian National University, Canberra, 0200, Australia..*

[b] *Research School of Physics and Engineering, Australian National University, Canberra, 0200, Australia.*

[c] *The School of Physical, Environmental and Mathematical Sciences, UNSW@ADFA, Canberra, 2600, Australia,*

The family of layered materials *MM*'PS_3 where *M*, *M*' = Mn, Fe, Ni, Mg, Zn etc shows a wide range of fascinating behaviour, magnetic and structural. The structure of the *MM*'PS_3 compounds is monoclinic and the in-plane coordination number is 3, relatively unusual. The family of compounds has been studied in the context of hydrogen sorption, fundamental magnetism, and a range of intercalation reactions, including the effect of intercalation on magnetism.

The material $Fe_{0.5}Mn_{0.5}PS_3$ is known to be a spin glass, and here we explore the magnetic a structural properties of some other 50:50 substituted compounds. In particular, $Fe_{0.5}Ni_{0.5}PS_3$ is shown to possess two magnetic phase transitions, one of which is highly hysteretic and suggestive of some form of magnetic glassiness.

WP18

Mobile Hole Dynamics in the Vicinity of an O(3) Quantum Critical Point

Michael Holt and Oleg.P. Sushkov

School of Physics, University of New South Wales, Sydney 2052, Australia.

Quantum Phase Transitions (QPT) between magnetically ordered and magnetically disordered states is a modern topic of great interest. A mobile hole injected in such a system is influenced by extreme quantum fluctuations that may completely change the properties of the hole. In the present work we consider a hole in the background of the bilayer Heisenberg antiferromagnet. Using the self-consistent Born approximation we study the properties of the hole in the vicinity of the QPT driven by the Heisenberg coupling between the planes. This study sheds light on the famous contradiction between the Fermi arcs and small hole pockets observed in angle-resolved photoemission spectroscopy and in quantum magnetic oscillation experiments in the cuprate high temperature superconductors.

WP19

Modelling Short-Range Order in Triglycine Sulphate

J.M. Hudspeth[a], D.J. Goossens[ab] and T.R. Welberry[b]

[a] *Research School of Physics and Engineering, Australian National University, Canberra, 0200, Australia.*

[b] *Research School of Chemistry, Australian National University, Canberra, 0200, Australia..*

Triglycine sulphate (TGS) [$(NH_2CH_2COOH)_3H_2SO_4$] is a hydrogen-bonded, ferroelectric with a transition temperature, T_C, of 47°C [1]. The transition is a reversible, second-order, order-disorder type, making it of fundamental interest to the field of phase transitions. While the average structure of TGS has been extensively studied, it does not provide sufficient information to understand how the molecules in the crystal are interacting and what the mechanism for the phase transition is. To gain more insight into what is happening in the real crystal, we need to look at the short-range order.

The program ZMC [2] models short-range order by creating a model crystal by in which the molecules can interact and bringing it to equilibrium using a Monte Carlo algorithm. Calculating the diffuse scattering pattern from the model crystal and comparing it with experimental data allows the validity of the model to be assessed. Here we present initial modeling of TGS and compare the results to diffuse x-ray scattering data.

[1] S. Hoshino, Y. Okaya and R. Pepinsky: *Phys. Rev.*, 1959, vol. 115, pp. 323-330.

[2] D.J. Goossens, A.P. Heerdegen, E.J. Chan and T.R. Welberry: *Metall. Mater. Trans. A*, 2010, vol. 41, pp. 1110-1118.

WP20

Studies of Near Surface Phosphorus Donors in Silicon via Electrically Detected Magnetic Resonance

W.D. Hutchison[a], P.G. Spizzirri[b], F. Hoehne[c], L.Y.S. Soo[a], L.K. Alexander[a], M.S. Brandt[c]

[a]*School of PEMS, University of New South Wales, ADFA, Canberra, ACT 2600, Australia.*

[b]*School of Physics, The University of Melbourne, Parkville, Victoria 3010, Australia.*

[c]*Walter Schottky Institute, Technical University of Munich, D-85748 Garching, Germany.*

The magnetic resonance of donors in semiconductors via their electron spin resonance (ESR) is well established. However, the sensitivity of conventional ESR is limited, requiring samples with 10^{10} donors or more. This problem can be overcome by detecting magnetic resonance via the effects of spin selection rules on other observables, such as charge transport.

Electrically detected magnetic resonance (EDMR) is a transport technique which measures the change in dc conductivity due to donor resonances. EDMR, first demonstrated on phosphorus doped silicon (Si:P) by Schmidt and Solomon [1], has the sensitivity to detect as few as 50 spins[2]. It is also particularly useful for the study of semiconductor interface defects and their influence on donors which are located in proximity. At Wagga2010 [3], we presented comparisons of EDMR results for Si:P devices with different surface preparations. We not only found a strong correlation between P and P_b charge trap signal strengths matching the postulated recombination mechanism requiring both these species[4,5], but also the surprising result of larger signal strengths from thermal oxides with lower areal trap densities. In this work, we further explore the underlying reasons for this counter intuitive signal enhancement as a function of trap density and present new data which shows continuing degradation of the silicon interface with time.

[1] J. Schmidt and I. Solomon, Compt. Rend. Paris **263**, 169 1966.

[2] D.R. McCamey, H. Huebl, M.S. Brandt, W.D. Hutchison, J.C. McCallum, R.G. Clark and A.R. Hamilton, Applied Physics Letters, **89** 182115-1 - 182115-3 (2006).

[3] W.D. Hutchison, P.G. Spizzirri, F. Hoehne and M.S. Brandt, paper 8**,** Proceedings of the 34rd ANZIP Condensed Matter and Materials (Wagga) Meeting, Waiheke 2010. http://www.aip.org.au/wagga2010/

[4] D. Kaplan, I. Solomon and N.F. Mott, *Journal de Physique – Lettres* **41** 159 (1976).

[5] F. Hoehne, H. Huebl, B. Galler, M. Stutzmann and M.S, Brandt, Phys. Rev. Lett. **104**, 046402 (2010).

WP21

New Sample Environments and Science Opportunities at the Bragg Institute

P. Imperia

The Bragg Institute, ANSTO, Lucas Heights, NSW Australia.

New sample environments are being developed for the neutron scattering facility at the Bragg Institute. The equipment in advanced engineering or manufacturing phases includes a 12 T vertical magnet, 20 mK dilution insert, 200 bar gas mixing and sorption system and a 10 bar 50 °C vapour delivery system.

This new equipment will be delivered and commissioned in 2011. It is likely this equipment will be already available for the next call for proposals for experiments at the Bragg Institute between September 2011 and March 2012.

In this presentation together with the newest projects, a review of recently commissioned equipment and their scientific cases will be presented. The details of the new equipment, time lines and examples of scientific applications at the neutron scattering facility made possible by the acquisition of this high level equipment will be discussed.

WP22

Time differential perturbed angular correlation spectroscopy of ^{100}Pd/Rh in rhenium and hafnium

W.J Kemp[a], Adurafimihan A. Abiona[a,*] , P. Kessler[b], R. Vianden[b], H. Timmers[a]

[(a)] School of Physical, Environmental and Mathematical Sciences, The University of New South Wales, Canberra Campus, ACT 2602, Canberra, Australia
[(b)] Helmholtz-Institut für Strahlen- und Kernphysik, Nußallee 14-16, 53115 Bonn, Germany
[(*)] On leave from Centre for Energy Research and Development, Obafemi Awolowo University, Ile-Ife, Nigeria

Time-differential angular correlation (TDPAC) spectroscopy is a nuclear technique of analysis that is used in the study of solid state physics. Measurements of the time dependence of the angular correlation pattern of two γ-rays in a γ-γ cascade, resulting from the hyperfine interaction of the intermediate nuclear state with a magnetic field or electric field gradient, provide information on the placement of atoms and atomic defects in the lattice environment proximate to the probe atom.

The 14 UD Pelletron accelerator at the Australian National University was used to synthesize ^{100}Pd/^{100}Rh probe nuclei, which were recoil-implanted into hafnium, rhenium, rhodium, antimony, titanium, tin and zinc foils, following the fusion evaporation reaction ^{92}Zr(^{12}C, 4n)^{100}Pd. Due to its complex synthesis, the interactions of this probe in many materials are not well known. For example, no data exist for rhenium and hafnium. The other metals have been studied for comparison. Results, such as the respective quadrupole coupling constants, will be presented and an outlook will be given.

.

WP23

Characterization of Nematic Liquid Crystals using Terahertz spectroscopy

M. Koeberle[1], E. Pogson[2], R. Jakoby[1] and R. A. Lewis[2]

[1]*Microwave Engineering, Technische Universität Darmstadt,*
Merckstraße 25, 64283 Darmstadt, Germany

[2]*Institute for Superconducting and Electronics Materials, University of Wollongong,*
Wollongong, New South Wales 2522, Australia.

Nematic Liquid Crystals (NLCs) are promising materials for tunable components like reconfigurable filters, phase shifters and antenna arrays at millimeter and submillimeter wave frequencies [1, 2]. As the exact knowledge of the material parameters – especially permittivity and dielectric losses – is necessary for the design and realization of such components terahertz (THz) spectroscopy has been used to characterize NLCs up to 1 THz. Permittivity as well as dielectric losses have been determined for different commercially available NLCs. The nematic temperature range and the temperature dependent permittivity and losses are measured. To exclude system based misleading results the characterization has not only been performed with a heterodyne continuous-wave THz system [3] but also with a THz time domain spectroscopy setup [4].

[1] T. Gobel, R. Meissner, A. Gaebler, M. Koeberle, S. Mueller and R. Jakoby, *Dual-frequency switching Liquid Crystal based tunable THz Filter*, Conference on Lasers and Electro-Optics, 2009.

[2] M. Koeberle, M. Hoefle, M. Chen, A. Penirschke and R. Jakoby, *Electrically Tunable Liquid Crystal Phase Shifter in Antipodal Finline Technology for Reconfigurable W-Band Vivaldi Antenna Array Concepts*, 5th European Conference on Antennas and Propagation, 2011 *[abstract submitted for review]*

[3] M. Koeberle, T. Göbel, D. Schönherr, S. Mueller, R. Jakoby, P. Meissner and H.-L. Hartnagel, *Material Characterization of Liquid Crystals at THz-Frequencies using a Free Space Measurement Setup*, German Microwave Conference, 2008.

[4] E. M. Pogson, R. A. Lewis, M. Koeberle and R. Jakoby, *Terahertz time-domain spectroscopy of nematic liquid crystals,* SPIE Nonlinear Optics and Applications IV, vol. 7728, 2010.

WP24

Decay width of the longitudinal magnon in the vicinity of an O(3) quantum critical point

Y. Kulik[a] and O.P. Sushkov[a]

[a] *School of Physics, The University of New South Wales, Sydney 2052, Australia.*

We consider an antiferromagnet in the vicinity of a quantum critical point at which there is a phase change between the magnetically ordered and the magnetically disordered phases. This can be observed experimentally in $TlCuCl_3$, where the quantum phase transition can be driven by hydrostatic pressure and/or by external magnetic field. Two transverse and one longitudinal magnetic excitations have been observed in the magnetically ordered phase. According to the experimental data, the longitudinal magnon has a substantial width, which has not been understood and has remained a puzzle. In the present work, we explain the mechanism for the width, calculate the width and relate the width with the Bose condensation of magnons observed in the magnetically disordered phase.

WP25

Topological Atoms in Crystals and their role in Crystalline Bonds

Philip S. Lavers
Institute for Superconducting & Electronic Materials
University of Wollongong, Innovation Campus
Squires Way, Fairy Meadow, NSW 2519, Australia

Two scalar functions of position (vector) $\mathbf{r}$ in real space within an infinite crystal, the electronic charge density distribution $\rho(\mathbf{r})$ and electrostatic potential distribution $V(\mathbf{r})$ are related by the Maxwell equation $\nabla \cdot \mathbf{E} = \frac{\rho(\mathbf{r})}{\epsilon_0}$ leading to $\nabla^2 V(\mathbf{r}) = \frac{\rho(\mathbf{r})}{\epsilon_0}$ and can be calculated one from the other. They can also be mapped quite accurately by experimental measurement - the former by X-ray diffraction and the latterby high energy electron diffraction [1].

The information contained in these distributions can be summarised in terms of the two "topological atoms" that can be calculated from them. The Electronic Charge Density atom (ECD atom) has been introduced by Bader [2] and the related Electrostatic Potential atom (ESP atom) has been introduced by Tsirelson and Ozerov [1]. These are described in the next section.

This paper describes bonding in a crystalline material in terms of these two types of topological atoms. A large proportion of crystalline materials are essentially ionic, but a small degree of covalency enhances bond strength and influences the material properties. The degrees of ionicity or covalency can be well displayed graphically from the relationships between the two types of atom for each elemental constituent. The paper gives examples to demonstrate the ideas graphically. The examples include several distinctive perovskites since the important perovskite structure is very much determined by the varying degrees of covalency within these essentially ionic crystals.

The author has developed computer routines to deal with the quantitative aspects of this approach, and charge transfer between atoms can be measured to give a more accurate result than Mulliken analysis. The Mulliken scheme's symmetrical allocation of overlap is arbitrary [3] and the overlap itself is dependent on the basis set, whereas the results presented here could in principle be derived from direct measurement.

In addition, a measure, being the electronic charge density at the bond critical point divided by the bond length, is proposed as a good proxy for the overlap or "hybridisation" or resonance of seperate electronic wave functions contributing to the various crystalline orbitals.

In effect this density functional theory approach is a way of examining the quantum mechanical phenomenon of bonding in crystals without resort to quantum mechanics.

TP1

Proximity effect on ion track etching in amorphous SiO_2

James Leslie, Briana Hillman, and Patrick Kluth

Department of Electronic Materials Engineering, Research School of Physics and Engineering, The Australian National University, Canberra ACT 0200, Australia.

As swift heavy ions pass through a material, they can disturb the structure in their path, leaving behind cylindrical damage zones a few nanometres in radius and microns in length, so called ion tracks. Often, the damaged zones show enhanced chemical etching compared to undamaged material, resulting in conical holes in the surface of the material, which can be imaged using scanning electron microscopy (SEM). An example of an SEM image of etched ion tracks in amorphous SiO_2, thermally grown on Si substrates, is provided in figure 1. The ion tracks were generated by irradiation with 185 MeV Au ions and subsequent chemical etching using HF. We have analysed a series of such SEM images of etched ion tracks in amorphous SiO_2, and statistically evaluated the influence of the proximity of the tracks on the etched track cross-section. We have found that adjacent tracks below a critical separation distance show smaller etched track cross-sections than isolated tracks, as shown by the graph in figure 2. This critical separation distance of 0.22 microns exceeds the etched track diameter of 0.18 microns, which is far greater than the actual 'unetched' track diameter of 0.05 microns. This effect is consistent with an influence of strain induced in the material during track formation on the etching rate of the material.

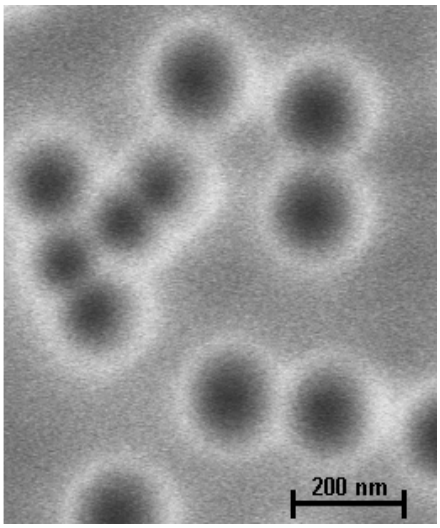

Figure 1: Example SEM image of etched ion tracks in a-SiO_2

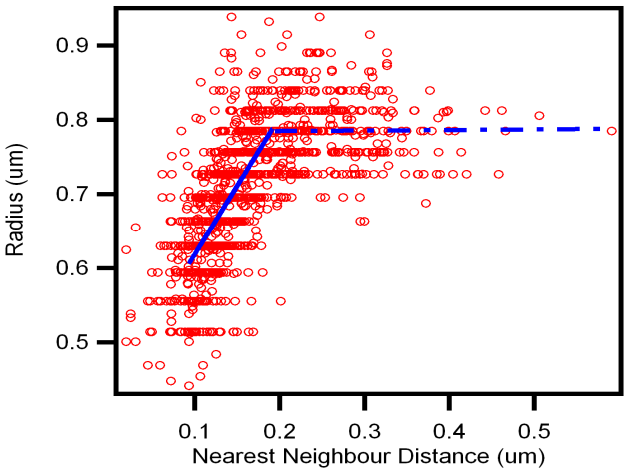

Figure 2: Graph of etched track radius vs distance to the nearest neighbor, and linear fits displaying the critical distance

TP2

Spin dynamics and Zeeman splitting of holes in a GaAs point contact

T. Li[a], O.P. Sushkov[a], U. Zuelicke[b]

[a] *School of Physics, University of New South Wales, NSW 2052, Australia.*

[b] *Institute of Fundamental Sciences, Massey University, PN 461, New Zealand.*

The strong spin-orbit coupling in GaAs (and other zinc-blende structures) leads to some interesting possibilities for the manipulation of spin with electric fields. A hole can be treated as a particle with spin 3/2 satisfying a Dirac-like equation which in 3D decouples into light-hole and heavy-hole states. In a confined system, the spin dynamics of holes is qualitatively different to that of electrons: conductance experiments indicate that the Zeeman splitting is highly anisotropic and depends on the interplay between the applied confinement and the nature of the valence band, and needs to be considered together with the surprisingly nontrivial nature of the transport in a 1D wire. As these features seem to underline properties of the crystal Hamiltonian that are absent (or negligible) for electrons, they make for a theory substantially more interesting, but less studied.

In the present work we consider mechanisms for the anisotropic Zeeman splitting and compare to the results of previous experiment.

TP3

On the atomic anisotropy of thermal expansion in bulk metallic glass

K.-D. Liss[a], D.D. Qu[b] , M. Reid[c] and J. Shen[b]

[a] *The Bragg Institute, Australian Nuclear Science and Technology Organisation, Lucas Heights, NSW 2234, Australia.*

[b] *State Key Laboratory of Advanced Welding Production Technology, Harbin Institute of Technology, Harbin 150001, China.*

[c] *Faculty of Engineering, University of Wollongong Wollongong, NSW 2522, Australia.*

Glass transition temperature and plastic yield strength are known to be correlated in metallic glasses. We have observed by in-situ synchrotron high energy X-ray diffraction anisotropy in the thermal expansion behavior of the nearest neighbor and second nearest neighbor atomic distances in the building blocks of Zr-Cu-Ni-Al based bulk metallic glass, leading inevitably to local shear stresses. Mechanical yielding of the latter on the atomic scale leads to the glass transition and the increase of the free volume. These experimental results uncover the mechanism, how glass transition and yield strength are linked. [1,2]

[1] Dongdong Qu, Klaus-Dieter Liss, Kun Yan, Mark Reid, Jonathan D. Almer, Yanbo Wang, Xiaozhou Liao, Jun Shen: *"On the atomic anisotropy of thermal expansion in bulk metallic glass"*, submitted for publication (2010).

[2] Dongdong Qu, Klaus-Dieter Liss and Jun Shen: *In Situ Diffraction Studies on Heating and Compression of Bulk Metallic Glasses"*, Symposium U: Bulk Metallic Glasses and their Applications, MRS Fall Meeting, Boston (2010).

TP4

Possible lubrication and temperature effects in the microscratching of polyethylene terephthalate

Yanyan Liu, Heiko Timmers

School of Physical, Environmental and Mathematical Sciences, The University of New South Wales, Canberra Campus, ADFA, Canberra, ACT 2600, Australia

Polyethylene terephthalate (PET) is a thermoplastic polymer which is used widely. It can exist in the form of an amorphous polymer (transparent) and as semi-crystalline polymer. Studies show that the tribological behaviour of polymers exhibits a strong dependence on the imposed friction condition [1]. The friction-induced heat results in a temperature increase in the surface layer during the sliding process [2]. Two temperatures are mainly studied when discussing the frictional temperature: environmental temperature and contact temperature [3-5]. Thus temperature and heat dissipation by a lubricant may also affect the depth and width of microscratches and associated wear debris particles.

In this project, the effect of environmental temperature on PET micro-scratch is investigated in order to understand the micrometer-scale wear mechanism of the polymer. Micro-scratching was conducted using a purpose-built micro-scratcher. The specimens of PET (Goodfellow Ltd.) were cut into squares (10 mm×10 mm ×1 mm). In a novel approach silicon cubic corner tips were cleaved from a silicon wafer to act as single scratching asperities.

Two scratch conditions (dry scratch and scratch in water) were carried out and different scratching environmental temperatures (9°C, 20°C, 73°C) were compared to investigate the effect of temperature on the tribological behavior of PET specimens. SEM imaging has shown that no detached wear debris adhered to the silicon cubic corner tip after scratching. However, there is some detached wear debris at the end of the scratch groove. Using Zum Gahr's formalism[6-7], it has been shown that there is no significant effect of environmental temperature and lubrication on the scratch dimensions.

[1] N.K. Myshkin, Tribology of polymers: Adhesion, friction, wear, and mass-transfer, *Tribol Int* 2005, 35: 910-921.
[2] G. Zhang, H. Yu, Temperature dependence of the tribological mechanisms of amorphous PEEK (polythereth erketone) under dry sliding conditions, *Acta Mater* 2008, 56:2182-2190.
[3] B.J. Briscoe, Friction and wear of polymer composites, *Amsterdam: Elsevier* 1986, 25-29
[4] J.M. Degrange, M.Thomine, Influence of viscoelasticity on the tribological behaviour of carbon black filled nitrile (NBR) for lip seal application, *Wear* 2005, 259:684-692.
[5] M Kalin, Influence of flash temperature on the tribological behaviour in low-speed sliding: a review, *Mater Sci Eng A* 2004, 374:390-397.
[6] M.F. Strond, H Wilman, The proportion of the groove volume removed as wear in abrasion of metals, *Brit.J.Appl.Phys*.1962, 13:173-178.
[7] K.H. Zum Gahr, Mircosturcture and wear of materials, *Elsevier Science Publishers B.V*., 1987.

TP5

Studies of magnetic nanoparticles formed in SiO_2 by ion implantation

A. E. Malik[a,b], W.D. Hutchison[a], K. Nishimura[c] and R.G. Elliman[b]

[a]*School of Physical, Environmental and Mathematical Sciences, The University of New South Wales at ADFA, Canberra ACT 2600.*

[b]*Electronic Materials Engineering Department, Research School of Physics and Engineering, Australian National University, Canberra, ACT 0200, Australia.*

[c]*Graduate School of Science and Engineering, University of Toyama, Toyama, Japan.*

Nanoparticles composed of magnetic metals such as Fe, Ni, Co and their alloys or compounds, are of great scientific and technological interest because their properties can differ from those of bulk materials as a direct consequence of their small physical dimensions and/or quantum confinement effects [1]. Such nanoparticles have many potential applications in areas as diverse as biotechnology, magnetic fluids, catalysis, magnetic resonance imaging and data storage. The latter application, which is the focus of the present study, typically requires a high density of small magnetic nanoparticles located in the near-surface region of protective matrix or thin-film. The ability to pattern arrays is also an advantage offered by the implantation technique.

At Wagga 2010, we outlined our work on synthesis of Ni, Co and Pt nanoparticles, embedded in silica layers thermally grown on silicon substrates, by the combination of ion implantation and post implantation annealing [2]. In this present paper we expand the work to include nanoparticles of Fe, Ni, Co and Pt together with various binary and ternary alloys. We also have expanded the range of thermal anneal conditions. Again the size and spatial distributions of the nanoparticles are determined from transmission electron microscopy of sample cross-sections and the crystal structure form glancing angle X-ray diffraction analysis. These results are correlated with SQUID magnetometry to elucidate emerging trends.

[1] L.G. Jacobsohn, M.E. Hawley, D.W. Cooke, M.F. Hundley, J.D. Thompson, R.K. Schulze and M. Nastasi, Journal of Applied Physics **96**, 8 (2004) 4444-4450.

[2] A. Malik, K. Belay, D. Llwellyn, W.D. Hutchison and R. Elliman, paper 7**,** Proceedings of the 34rd Annual ANZIP Condensed Matter and Materials Meeting, Waiheke 2010. http://www.aip.org.au/wagga2010/

TP6

Effect of hydrogen back pressure on de/rehydrogenaiton behavior of $LiBH_4$-MgH_2 system and the role of additive toward to enhanced hydrogen sorption properties

Jianfeng Mao, Zaiping Guo, Huakun Liu

Institute for Superconducting and Electronic Materials, University of Wollongong, Australia

Metal hydrides are considered to be one of the most promising materials for reversible hydrogen storage. However, no single metal hydride or complex hydride can fulfil all the requirements as on-board hydrogen storage medium for mobile applications due to the drawbacks in de/rehydrogenation kinetics or thermodynamics. Against this background, high capacity reactive hydride composites were developed through combining two or more hydrides to form a new compound upon dehydrogenation, thereby lowering the overall reaction enthalpy. One of the most promising systems of this kind is the $LiBH_4$-MgH_2 composite, reacting to form LiH, MgB_2 and H_2 during desorption according to 2LiBH4 + MgH_2 $\rightarrow$ 2LiH + MgB_2 + 4H_2, the reaction enthalpy is 46 kJ/mol H_2, which is much lower than for the decomposition of pure $LiBH_4$ (74 kJ/mol H_2). Also, the reversibility of the reaction is proven previously. However, the reaction kinetics is very slow, needed 100 h to attain equilibrium for direct measurements even at 400 °C. More importantly, further research reveals that the dehydriding reaction proceeds by a different mechanism, that is, MgH_2 decomposes into Mg and H_2 before $LiBH_4$ is dehydrogenated according to MgH_2 + 2$LiBH_4$ $\rightarrow$ 2LiH + Mg + 2B + 4H2. The reaction is hard to reverse because the B-B bond is likely to be more stable than the B-Mg bond. Motivated by these considerations, we first discussed the effect of hydrogen back pressure on the de/rehydrogenation kinetics of $LiBH_4$-MgH_2 system. The results indicate that the lower hydrogen back pressure allow faster desorption kinetics but deserve much slow absorption kinetics due to the formation of boron. In contrast, the applied higher hydrogen back pressure remarkably promotes the formation of MgB_2, the formation of MgB_2 plays a crucial role in enhancing the absorption kinetics and increasing the reversible hydrogen storage capacity of these composites. However the formation of MgB_2 is achieved with penalty of much slow desorption kinetics. Furthermore, the effect of NbF_5 on the system at different hydrogen back pressure is investigated toward to improve its sorption kinetics and to achieve a full reversible system.

TP7

Chemical control of gate length in lateral wrap-gated InAs nanowire FETs

A.P. Micolich[a,b], K. Storm[b], G. Nylund[b] and L. Samuelson[b]

[a] School of Physics, University of New South Wales, Sydney NSW 2052, Australia.

[b] Solid State Physics/Nanometer Structure Consortium, Lund University, S221-00 Lund, Sweden.

Self-assembled semiconductor nanowires offer great promise for future device applications. While vertically oriented nanowire field effect transistors (NW-FETs) have received much attention [1], most NW-FETs used for fundamental transport and quantum device studies are instead oriented laterally on a semiconductor substrate [2-4]. In lateral NW-FETs, gating is achieved using a heavily doped Si substrate [2], insulated metal gates directly underneath the nanowire [3], or top-gates deposited over an oxide-coated nanowire [4]. Each results in a gate-channel capacitance that is difficult to calculate, and which produces an inhomogeneous charge density within the nanowire [5]. The ideal configuration is a concentric metal 'wrap-gate', but it is a challenging goal in the lateral orientation, because depositing gate metal underneath a nanowire already sitting laterally on a substrate is a formidable undertaking, and using a nanowire where the wrap-gate exists prior to deposition onto a substrate entails the difficulty of exposing the ends of the nanowire to make contacts that are not electrically shorted to the wrap-gate.

We report a method for producing laterally oriented wrap-gated NW-FETs that provides exquisite control over the gate length via a single wet etch step, eliminating the need for additional lithography beyond that required to define the source/drain contacts and gate lead. Our devices provide stronger, more symmetric gating of the nanowire, operate at temperatures between 300 to 4 Kelvin, and offer new opportunities in applications ranging from studies of one-dimensional quantum transport through to chemical and biological sensing.

[1] C. Thelander *et al.*, *Materials Today* **9(10)**, 28 (2006).

[2] X. Duan *et al.*, *Nature* **409**, 66 (2001).

[3] C. Fasth *et al.*, *Nano Letters* **5(7)**, 1487 (2005).A.

[4] A. Pfund *et al.*, *Applied Physics Letters* **89**, 252106 (2006).

[5] D.R. Khanal and J. Wu, *Nano Letters* **7(9)**, 2778 (2007).

TP8

High Temperature Thermodynamics of the Multiferroic $Ni_3V_2O_8$

J. Oitmaa [a] and A. Brooks Harris [b]

[a] School of Physics,The University of New South Wales, Sydney NSW 2052, Australia.

[b] Department of Physics and Astronomy, University of Pennsylvania, Philadelphia, U.S.A.

The nickel vanadate $Ni_3V_2O_8$ is a much studied material [1], with magnetic transitions at 9.1K, 6.3K, 3.9K between different phases, including a 'multiferroic' phases which shows simultaneous ferroelectric and magnetic order.,

The material itself is rather complex, with 6 magnetic Ni^{++} S=1 ions per orthorhombic unit cell, forming a structure of coupled 'Kagome staircase' planes. A first-principles electronic structure calculation (LDA+U) [1] has identified as many as 12 different exchange constants, of which 5 appear to be dominant.

In the present work we use high-temperature series expansions [2] to compute the specific heat and magnetic susceptibility for a 5-parameter Heisenberg model of this material. The results are compared with experimental data [3] to test the adequacy of the model and to try to refine the values of the exchange parameters.

[1] T. Yildirim et al., J.Phys.Condens.Matter **20**, 434214 (2008).

[2] J. Oitmaa, C.J. Hamer and W. Zheng, Series Expansions for Strongly Interacting Lattice Models (Cambridge, 2006) .

[3] N. Rogado et al., Solid State Commun. **124**, 229 (2002), and G. Lawes, *private communication.*

TP9

Does the Quantum Compass Model in 3D Have a Phase Transition?

J. Oitmaa and C.J. Hamer

School of Physics, The University of New South Wales, Sydney NSW 2052, Australia.

Quantum compass models are spin models with nearest neighbour coupling of the form $J_\alpha S_i^\alpha S_j^\alpha$ where α (= x,y,z) depends on the spatial direction of the particular link or bond. This then implies a coupling between the spin space and the physical space of the lattice. Such models were first introduced, and have often been used, to describe orbital ordering in transition metal compounds [1]. More recently they have been used as models of p + ip superconducting arrays, and it has been argued that such arrays can provide fault-tolerant qubits for quantum information systems [2].

Recent Quantum Monte Carlo studies of such a model on the 2D square lattice [3] have found strong evidence for a finite temperature critical point of the 2D Ising universality class, separating a high T disordered phase from a low T phase of orientational or 'nematic' nature. The corresponding 3D model on the simple cubic lattice has not been studied previously.

We address this question using the standard method of high temperature expansions. For the 2D case our results show clear evidence for a finite temperature transition, in agreement with previous work. However, for the 3D case our series show no signature of a transition [4], and we are led to conjecture that there is no finite temperature nematic phase. While at first sight this seems surprising, it is in fact consistent with the rather peculiar nature of correlations in this model.

[1] J. van der Brink, New J.Phys. **6**, 201 (2004), and references therein.

[2] Z. Nussinov and E. Fradkin, Phys.Rev.B**71**, 195120 (2005).

[3] S. Wenzel, W. Janke and A. Lauchli, Phys.Rev.E**81**, 066702 (2010).

[4] J. Oitmaa and C.J. Hamer, Phys.Rev.B (2011), in press.

TP10

Scaling of Critical Temperature and Ground State Magnetization near a Quantum Phase Transition

J. Oitmaa and O.P. Sushkov

School of Physics, The University of New South Wales, Sydney NSW 2052, Australia.

A number of systems exist which show long-range magnetic order below some critical temperature $T_c(g)$ and where T_c decreases to zero as some control parameter $g \rightarrow g_c$, corresponding to a quantum critical point in the ground state. An example is $TlCuCl_3$ [1], in which the quantum critical point is driven by pressure, and separates an antiferromagnetic Neel phase from a quantum dimer phase.

We consider a simple model spin system which mimics this behaviour. The model is a spin-1/2 cubic antiferromagnet with bonds of strength J and gJ. Using series expansions at T=0 and at high T [2], we compute both the Neel temperature $T_N(g)$ and the ground state magnetization $M_0(g)$. These are observed to scale in a similar way near the quantum critical point. We believe this is generic and represents a universal feature of quantum phase transitions [3].

[1] Ch. Ruegg et al., Phys.Rev.Lett. **100**, 205701 (2008).

[2] J. Oitmaa, C.J. Hamer and W. Zheng Series Expansion Methods for Strongly Interacting Lattice Models (Cambridge, 2006).

[3] S. Sachdev, *Quantum Phase Transitions* (Cambridge, 1999).

TP11

Strain to selectively excite certain orientations of NV centres in diamond

L.J. Rogers[a,b], K.R. Ferguson[b] and N.B. Manson[b]

[a] *Faculty of Science and Mathematics, Avondale College, Cooranbong 2265, NSW, Australia.*

[b] *Laser Physics Centre, RSPE, Australian National University, Canberra 0200.*

The negatively-charged Nitrogen-Vacancy (NV) defect centre in diamond is of increasing interest for many quantum information and metrology applications. Due to the atomic structure of diamond, there are four possible orientations of the NV centre which has C_{3v} symmetry. By examining both the primary 637nm visible transition as well as the 1042nm infrared transition, we have been able to selectively excite and measure individual sets of identical orientations. These results yield an unambiguous designation for the components of the strain-split infrared zero-phonon line, and the technique may be more generally useful for ensemble studies.

TP12

Ambient and high pressure μSR measurements on the ferromagnetic superconductor UGe_2

S. Sakarya[a], P. C. M. Gubbens[a], A. Yaouanc[b], P. Dalmas de R´eotier[b], D. Andreica[c], A. Amato[d], U. Zimmermann[d], N. H. van Dijk[a], E. Br¨uck[a], Y. Huang[e], T. Gortenmulder[e], A. D. Hillier[f], and P. J. C. King[f]

[a]*FAME, R3, Faculty of Applied Sciences, Delft University of Technology, 2629JB Delft, The Netherlands*
[b]*CEA/DSM/Institut Nanosciences et Cryog´enie, 38054 Grenoble, France*
[c]*Laboratory for Muon-Spin Spectroscopy, Paul Scherrer Institute, 5232 Villigen-PSI, Switzerland*
and Faculty of Physics, Babes-Bolyai University, 400084 Cluj-Napoca, Romania
[d]*Laboratory for Muon-Spin Spectroscopy, Paul Scherrer Institute, 5232 Villigen-PSI, Switzerland*
[e]*van der Waals-Zeeman Laboratorium, Universiteit van Amsterdam, 1018XE Amsterdam, The Netherlands*
[f]*ISIS Facility, Rutherford Appleton Laboratory, Chilton, Didcot OX11 0QX, United Kingdom*

Results of a detailed investigation of the ferromagnetic superconductor UGe_2 using positive muon spin rotation and relaxation experimental techniques. We observe two muon stopping sites. The most interesting result is the relatively large value of the elements of the hyperfine tensor for one of the two localisation sites. At this site the muon est quite sensitive to the conduction electron properties. The pressure and temperature dependences of the frequencies and related spin-spin relaxation rates are remarkable. The study shows that the transition from the weakly to the strongly polarized magnetic (WP-SP) phases is still observable at TX ≃ 3K under a pressure of 1.33 GPa. Thus this transition survives at higher pressures than previously believed. Although the magnetic phase transition from the paramagnetic to the ferromagnetic states is first order at that pressure, there is no magnetic phase separation. The temperature TX at 1.0 GPa corresponds clearly to a thermodynamic phase transition, rather than a cross-over. No such statement can be given reliably at lower pressure. A substantial shrinking of the component along the easy axis of diagonal hyperfine tensor, at the muon site where it is large, is observed in the SP phase relative to the WP phase. This is clearly detected at 0.85 GPa and below, including ambient pressure. This corresponds to an appreciable decrease of the electronic density at the Fermi level in the SP phase. We do not detect any signature of the spontaneous vortex lattice down to a temperature of about half of the superconducting temperature at 1.25 and 1.33 GPa. This allows us to put a lower bound on the value of one of the component of the London penetration depth tensor, which is at 0.3K: ≥ 270 nm.

TP13

Small Angle Scattering: instrumentation and applications to study various materials at the nanoscale

A. Sokolova

Bragg institute, Australian Nuclear Science and Technology Organization, Sydney, Australia

Small Angle Scattering (SAS) technique is a powerful unique tool to study various materials. The method provides structural information on condensed phases of different nature at resolution level ranging from about 1 to about hundreds of nanometers. Both, X-rays and neutrons can be utilized in SAS method.

Number of large facilities provides access to SAS X-rays (SAXS) and neutron (SANS) instruments. Australian Nuclear Science and technology Organization (ANSTO, Sydney, Australia) successfully operates one SANS instrument Quokka and recently commenced construction of the second SANS instrument, Bilby.

The presentation will be focused on possibilities to use SAS neutron technique in applied science, in particular in biotechnology and medicine, in metal and in magnetic devices industry. The advantages and limitations of the method will be underlined. The requirements to samples preparation will be listed. The capabilities of two instruments at ANSTO, Quokka and Bilby as well as a way to get access for use of the instruments will be described.

TP14

Thermal hysteresis of the ^{169}Tm quadrupole interaction in orthorhombic thulium manganite

G.A. Stewart[a], H. Salama[a], A. Mulders[a], D. Scott[b] and H.StC. O'Neill[b]

[a] *School of Physical, Environmental & Mathematical Sciences, University of New South Wales, Australian Defence Force Academy, Canberra, ACT 2600, Australia.*

[b] *Research School of Earth Sciences, Australian National University, Canberra, Australia 2100.*

Magneto-electric multiferroics are currently a hot research topic because of their potential technological application in data storage and switching devices. The orthorhombic phase of $TmMnO_3$ orders at T_N = 41 K with an incommensurate magnetic structure which locks into a commensurate *E*-type structure at the lower temperature of T_C = 32 K. Pomkjakushin *et al*. [1] recently demonstrated that this onset of collinear magnetic order induces ferroelectricity with an electric polarization larger than observed for any other orthorhombic manganite. Using ^{169}Tm-Mössbauer spectroscopy, we were able to show that the transition to commensurate magnetic order is also accompanied by the emergence of a weak exchange interaction at the Tm^{3+} site, manifested as a subtle magnetic broadening of the Mössbauer absorption lines [2]. A further observation was that the transition is accompanied by a sharp increase in the quadrupole interaction strength at the ^{169}Tm nuclei. Given that the temperature-dependent, 4f-shell contribution to the electric field gradient at the nucleus involves a thermal average over the crystal field levels, it is unusual to observe such jumps. We report here on more recent^{169}Tm-Mössbauer data recorded with a higher density of data points. The outcome of these measurements is that the jump in the quadrupole interaction strength has been confirmed. Moreover, it was possible to observe the thermal hysteresis of the electric polarization via the temperature dependence of the quadrupole splitting. We believe that this is the first time that such a phenomenon has been observed using ^{169}Tm-Mössbauer spectroscopy, which highlights the magnitude of the magneto-electric effect in o-$TmMnO_3$. This work was supported by AINSE through ALNGRA10137.

[1] V.Yu. Pomjakushin et al., *New J. Phys.* **11**, 043019 (2009).

[2] H.A. Salama, G.A. Stewart, W.D. Hutchison, K. Nishimura, D. R. Scott and H. StC. O'Neill, *Solid State Commun*. **150**, 289 (2010).

TP15

Phase relationships in the PtAI2-AuAI2 system

S. Supansomboon, A. Dowd and M.B. Cortie

Institute for Nanoscale Technology, University of Technology Sydney, PO Box 123, Broadway, NSW2007, Australia.

The intermetallic compounds $PtAl_2$ and $AuAl_2$ are fully metallic but have bright colours, yellow for $PtAl_2$ [1] and purple for $AuAl_2$ [2]. It has been predicted that nanostructures of $AuAl_2$ should manifest a localized surface plasmon resonance [3]. This raises the interesting issues of (1) whether mixed microstructures of these two compounds could be used to tune the colour of a bulk substance between these two coloured end-points and (2) whether nanoscale composites or alloys of these two compounds would have a tunable localized surface plasmon resonance.

The compounds share the same c*F*12 (Pearson symbol) crystal structure and have similar physical properties. Furthermore, given the rather similar electronegativity and atomic diameter of Pt and Au, it might be expected that the two compounds would exhibit unlimited mutual solubility. However, no Pt-Au-Al ternary section appears to be available in the literature so the nature of the microstructures along the isopleth connecting these two compounds was unknown. We fabricated a range of nanoscale $PtAl_2/AuAl_2$ diffusion couples by magnetron sputtering onto inert substrates. The resulting structures were characterized in terms of physical morphology, chemical composition and optical properties. Our conclusion is that the two compounds are nearly mutually insoluble. This rules out alloying as a means to control dielectric function, however, nanoscale duplex microstructures comprised of these two compounds will still have an 'effective' dielectric function that is different from that of the components. We explore the possibilities inherent in such a chemical inhomogeneous 'meta-material'.

[1] J. Hurly and P. T. Wedepohl, *J. Mater. Sci.* **28**, 5648-5653 (1993)

[2] C. Cretu and E. van der Lingen, *Gold Bull.* **32**, 115-126 (1999)

[3] S. Supansomboon, A. Maaroof and M. B. Cortie, *Gold Bull.* **41**, 296-304 (2008)

TP16

Surface dynamics during Langmuir evaporation of GaAs

W. X. Tang[a], C. X. Zheng[a], Z. Y. Zhou[a], D. E. Jesson[a], J. Tersoff[b]

[a] *School of Physics, Monash University, Victoria 3800, Australia*

[b] *IBM Research Division, T. J. Watson Research Center, Yorktown Heights, NY 10598, USA*

The formation of Ga droplets during evaporation has been studied for decades, and recently Ga droplets have been applied in nanofabrication via droplet epitaxy. We will present recent in-situ studies of Langmuir evaporation of GaAs (001) using our novel surface electron microscopy [1-4].

First, we find that Ga droplets spontaneously run across the surface during Langmuir evaporation, This is driven by a disequilibrium between the droplet and the surrounding surface. Consequently at T_C, when the surface and droplets are in equilibrium, the motion stops. This intrinsic motions retained, even after evaporation of hundreds of atomic layers of the crystal and has important technological consequences for extensions of the droplet epitaxy technique [2].

In addition, striking bursts of 'daughter' droplet nucleation occur during the coalescence of large 'parent' droplets. This unexpected behavior results in a strong coupling between morphology and evaporation which has no direct analogy in single-component systems such as Si. These observations imply a morphology dependent T_C and we will demonstrate how this new concept can be used to position quantum structures by combining droplet epitaxy methods with standard lithography [3]. The mechanism of daughter droplet formation via coalescence also has major consequences for the evolving droplet size distribution.

Finally, we reveal how an external As flux directly controls T_C. A sensitive, real-space method based on Ga droplet stability is used to measure the flux dependence of T_C. The results are consistent with a simple model for surface evaporation under As flux which has direct application in MBE and surface preparation

[1] J. Tersoff, D. E. Jesson and W. X. Tang, *Science* **324** (2009) 236.
[2] J. Tersoff, D. E. Jesson and W. X. Tang, *Phys. Rev. Lett.* **105** (2010) 035702.
[3] Z. Y. Zhou, C. X. Zheng, W. X. Tang, D. E. Jesson and J. Tersoff, *Appl. Phys. Lett.* **97** (2010) 121912.

TP17

From Radiation Damage, through Minerals and Gemstones, to Art, with EPR

G.J.Troup[a], D.R.Hutton[a], J.Boas[a], A.Casini[b], M.Picollo[b], and Robyn Slogget[c]

[a] *School of Physics, Monash University Victoria 3800, Australia*

[b] *Consiglio Nazionale Ricerrche, Florence, Italy*

[c] *MelbourneUniversity, Victoria Australia*

In the spirit of celebrating the 50th anniversary of Monash University, this work summarises the research done by the EPR (Electron Paramagnetic Resonance) group of the Physics Department., Monash University, since its foundation in 1961 by G,Troup (lecturer then) and J.Thyer (Ph.D.student then), with a project involving **AINSE**: radiation damage in BeO. Ph.D.student D.Hutton commenced work on minerals and gemstones, initially to find possible new maser materials. As other students arrived, this work swelled into gemstone identification, and the investigation in various compounds (e.g., Olivines: Dr J.Creer), of their antiferromagnetism, for applications in millimeter wave technology. Magnetic structure, if unknown, was determined by neutron scattering (**AINSE**). Two years negotiation with the Argyle Co. led to EPR investigation of their diamonds: diamond sources give unique sets of centres observable by EPR. A period of Study Leave in Florence, Italy, with a laboratory of the Italian National Research Council (**CNR**) convinced the group that EPR could be applied to the identification of paint pigments in renaissance and later paintings: most pigments are mineral, and later synthetics should have different spectra. This proved to be true, despite suspected difficulties with powder spectra. A local collaboration was commenced with the conservation centre at the Ian Potter Gallery, Melbourne University, which asked could we distinguish Australian ochres from imported ones, since some painters were using the latter in paintings they claimed were Aboriginal. EPR did distinguish: the Australian ochres all had huge *radiation damage* signals in comparison to the imported ones! The scam was stopped.

All mentioned projects will be briefly treated with comments, and/or relevant spectra. To commence this work with radiation damage, and to end with it, is also a tribute to our long cooperation with **AINSE**. The diagram shows the EPR spectrum of a North Australian yellow ochre: the large sharp feature is from radiation damage. Horizontal.axis, magnetic field: centre 2 kG, sweep 4kG. vertical.axis, signal intensity.

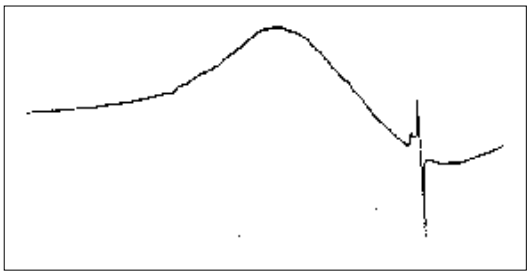

TP18

Magnetic Structures of Pr1-xLuxMn2Ge2 Compounds (x=0.2 and 0.4)

J.L. Wang[a,b,c], A.J. Studer[b], S.J. Campbell[c], S.J. Kennedy[b] , R. Zeng[a] and S.X. Dou[a]

[a]*ISEM, University of Wollongong, NSW 2522,*

[b]*Bragg Institute, ANSTO, Lucas Heights, NSW 2234,*

[c]*School of Physical, Environmental and Mathematical Sciences, UNSW@ADFA, ACT 2600*

Following our previous investigation of magnetic phase transitions in $Pr_{1-x}Lu_xMn_2Ge_2$ [1], the magnetic structures of $Pr_{1-x}Lu_xMn_2Ge_2$ (x=0.2; 0.4) have been investigated over the temperature range (10-450 K) using the high intensity diffractometer Wombat at OPAL. Four magnetic transitions have each been detected for both $Pr_{0.8}Lu_{0.2}Mn_2Ge_2$ and $Pr_{0.6}Lu_{0.4}Mn_2Ge_2$. The behaviour of successive magnetic transitions and structures is governed by the critical interplay of the lattice dimensions of the bct structure and interlayer and intralayer exchange interactions; here we present an overview of the effect of replacing Pr atoms with smaller Lu atoms leading to a complex series of magnetic states.

With decreasing temperature, $Pr_{0.8}Lu_{0.2}Mn_2Ge_2$ first changes from paramagnetism (PM) to intralayer antiferromagnetism (AFl) at T_N^{intra}~397 K and then to canted ferromagnetic ordering (Fmc) below T_C^{inter} ~ 330 K. A transition from F*mc* to the lower temperature conical spin structure (F*mi*) occurs at $T_{c/c}$~192 K. On further reduction in temperature, the transition at T_C^{Pr}=35 K (with related enhancement in magnetization) is assigned to the additional ferromagnetic contribution of the Pr sublattice, leading to Fmc+F(Pr) with the combination of ordering in the Mn and Pr sublattices. By comparison, for $Pr_{0.6}Lu_{0.4}Mn_2Ge_2$, the transition from PM to intralayer AFl occurs at T_N^{intra}~375 K while the canted Fmc state starts to form at T_C^{inter} ~ 321 K. With further decrease in temperature, $Pr_{0.6}Lu_{0.4}Mn_2Ge_2$ changes from Fmc to canted antiferromagnetic ordering (AFmc) at T_N^{inter}~ 172 K. The final re-entrant ferromagnetic state (Fmc+F(Pr) takes place at T_C^{Pr} ~31 K.

[1] J.L. Wang, S.J. Campbell, A.J. Studer, M. Avdeev, R. Zeng and S.X. Dou, J. Phys.: Condens. Matter 21, 124217 (2009).

TP19

Polymer Particle Production and Dispersion in Knee Prostheses

J.A. Warner[a], L.G. Gladkis[a], A. E. Kiss[a], J. Young[b] P. N. Smith[c], J. Scarvell[c], and H.Timmers[a]

[a] *School of Physical, Environmental and Mathematical Sciences, The University of New South Wales, Canberra Campus, ACT 2600, Australia.*

[b] *Aerospace, Civil & Mechanical Engineering, The University of New South Wales, Canberra Campus, ACT 2600, Australia.*

[c] *Trauma and Orthopaedic Research Unit, The Canberra Hospital, PO BOX 11, Woden, ACT 2606, Australia.*

While ultra-high molecular weight polyethylene (UHMWPE) has become the preferred bearing material in knee prostheses, the debris in particulate form can have harmful biological effects. Therefore the sensitive measurement of tibial insert wear rates is vital in regards to assessing the efficacy of various prosthetic designs. Current techniques remain insensitive to small amounts of wear, and are unable to measure local wear on specific tibial insert locations.

The direct ion implantation of In-111 to a depth of 200 nm in UHMWPE permits the investigation of the initial 'bedding in' phase for a model wheel-on-polymer system. During this phase, it has been shown that there is a two-way transfer of debris between the metal and the polymer surfaces, with a stochastic dropout to the lubricant. Computation Fluid Dynamic (CFD) simulations have been created and run for a wheel-on-polymer sliding situation. This simulation is consistent with the experimental results as it shows the constant re-entry of debris particles into the sliding interface once dispersed into the lubricant.

Further depths, up to 5 μm, have been labeled via the recoil implantation of the radioisotope tracers Ru-97, Pd-100, Rh-100, and Rh-101m into UHMWPE. This technique has been demonstrated to allow independent quantification of removed debris through multiple radioisotope tracers, while minimizing the fluence. *In vitro* wear experiments have been conducted with a state-of-the-art knee simulator and the backside wear rate has been measured to be (8.5 ± 1.7) mm^3 per 10^6 gait cycles, which is consistent with other *in vitro* experimental measurements using gravimetric methods. The results conclude the non-linear initial 'bedding in' phase is completed before 300,000 gait cycles. The removed debris destinations from the tibial insert were shown to split between the lubricant (53 ± 3) % and the metal tibial tray (48 ± 3) %.

TP20

$M_{(n+1)}AX_n$ Phases are they tolerant/resistant to damage

K.R. Whittle[a], D.P. Riley[a], M.G. Blackford[a], R.D. Aughterson[a], S. Moricca[a], G.R. Lumpkin[a] and N.J. Zaluzec[b]

[a] *Institute of Materials Engineering, ANSTO, Locked Bag 2001, Kirrawee DC, NSW, 2232, Australia*

[b] *Materials Science Division, Argonne National Laboratory, 9700 South Cass Avenue, Argonne, IL 60439, USA*

Ternary carbide materials have been proposed as having applications within the future nuclear technologies, both fusion (ITER/DEMO) and fission (GenIV). These new designs require a material to have the ability to tolerate radiation damage to high levels, with a high level of predictability. As part of such a process two systems, specifically Ti_3AlC_2 and Ti_3SiC_2 have been studied to determine their radiation tolerance, using in-situ ion beam irradiation with 1 MeV Xe ions, coupled with transmission electron microscopy. Irradiations have shown that both systems show little amorphisation at 300K up to doses of at least 6.25 x 10^{15} ions cm^{-2} (~28-30 dpa). However, there is a subtle difference between Ti_3AlC_2 and Ti_3SiC_2, with Ti_3SiC_2 showing more evidence for damage. Further irradiations using 500 KeV Xe to fluences equivalent to 100 dpa have also been undertaken, with crystalline material visible and evidence of recrystallisation. Explanations and possible mechanisms for recovery from damage are presented, along with implications for future potential uses.

TP21

The role of free volume in the tradeoff between high water permeability and high permeability selectivity of polymeric desalination membranes

Wei Xie[a], Hao Ju[b], James I. Mardel[c], Anita J. Hill[c],
James E. McGrath[d] and Benny D. Freeman[a]
[a]*University of Texas at Austin, Center for Energy and Environmental Resources, Austin, TX 78758, USA.*
[b]*The Dow Chemical Company, Materials Science and Engineering, Midland, MI 48640, USA.*
[c]*CSIRO Materials Science and Engineering, South Clayton MDC, Clayton, Vic. 3169, Australia.*
[d]*Virginia Polytechnic Institute and State University, Macromolecules and Interfaces Institute, Blacksburg, VA 24061, USA.*

Free volume plays a central role in determining the transport properties of small molecules in polymers. Polymeric membranes are becoming the technology of choice for water desalination because they are cost-effective, have a small footprint, and are simple to operate and maintain. Commercial reverse osmosis (RO) membranes are capable of rejecting more than 99% of ions such as Na^+ and other contaminants to produce potable water. This paper examines the role of free volume in the tradeoff between high water permeability and high permeability selectivity of hydrated polymers.

One part of this paper examines new chlorine stable membrane materials developed by McGrath et al. based on sulfonated poly(arylene ether sulfone) with tailored hydrophilicity, and in consequence, tailored water and salt transport properties. The free volume of membranes in the dry and hydrated states is measured and correlated with transport properties. The balance between high water permeability and high permeability selectivity is related to the free volume of the hydrated polymers. The other part of this paper addresses the use of poly(ethylene oxide) (PEO)-based polymers as coatings for reverse osmosis membranes. Such hydrogel coatings may reduce surface roughness and control surface chemistry, rendering the surface more hydrophilic and endowing it with enhanced resistance towards organic foulants. Salt diffusivity and permeability in these hydrogel coatings can be predicted using a free volume model. Free volume in hydrated crosslinked PEO coatings is examined using positron annihilation lifetime spectroscopy (PALS), and the results are compared with experiment and theory. Coatings with higher free volume generally exhibit higher NaCl and water permeability, but lower permeability selectivity for water over NaCl, indicating a distinct tradeoff between water permeability and water/NaCl selectivity.

TP22

Electrospinning Technology Used to Synthesize Nanomaterials for Lithium-ion batteries

Peng Zhang[*a], Zaiping Guo[**ab], Huakun Liu[a]
[a.] *Institute for Superconducting & Electronic Materials, University of Wollongong, NSW 2522, Australia;*
[b.] *School of Mechanical, Materials & Mechatronic Engineering, University of Wollongong, NSW 2522, Australia;*
[*] *Tel.: +61-2-4298-1485; Email: pz898@uow.edu.au*
[**] *Tel.: +61-2-4221-5225; Fax: +61-2-4221-5731. Email: zguo@uow.edu.au*

Lithium-ion batteries are widely applied as the power source for mobile devices and required for applications in hybrid electric vehicles [1]. Transition metal oxides, (such as CoO, NiO, Co_3O_4 and CuO), which can reversibly react with lithium are the most appealing and competitive materials for lithium-ion batteries [2]. The disadvantage of high initial capacity loss and poor cycling performance restrict the application of lithium-ion batteries [3]. To improve electrode capacity and rate capability, some studies proposed to synthesize materials with porous or one-dimantional structure which has high specific surface area [4-6]. Electrostatic spray deposition (ESD) is a unique method to create promising morphologies [4]. By carefully select the solvent, we can either create one-dimentian nanowires or nanotubes, or we can produce 3-d porous structure. And by setting different electrospinning parameters, like accelerating voltage, flow speed, and depositing distance, it is possible to control the size of porous or the diameter of the nanowires. In our paper, we discussed the electrospinning technology and its application in synthesizing nanomaterials for lithium ion batteries.

[1] J.L. Shui, Y. Yu, X.F. Yang, C.H. Chen, Electrochemistry Communication 8 (2006) 1087-1091.
[2] P. Poizot, S. Laruelle, S. Grugeon, L. Dupont, J-M. Tarascon, Nature 407 (2000) 496-499.
[3] Y. Yu, Y. Shi, C. Chen, Nanotechnology 18 (2007) 055706.
[4] J.L. Shui, Y. Yu, C.H. Chen, Applied Surface Science 253 (2006) 2379-2385.
[5] Y. Yu, C.H. Chen, Y. Shi, Advanced Materials 19 (2007) 993-997.
[6] Y. Yu, J.L. Shui, S. Xie, C.H. Chen, Aerosol Science and Technology 39 (2005) 276-281.

TP23

Design and Application of a III-V Surface Electron Microscope

C. X. Zheng[a], Z. Y. Zhou[a], W. X. Tang[a], D. E. Jesson[a], J. Tersoff[b], and B. A. Joyce[c]
[a] *School of Physics, Monash University, Victoria 3800, Australia*
[b] *IBM Research Division, T. J. Watson Research Center, Yorktown Heights, NY 10598, USA*
[c] *Department of Physics, Blackett Laboratory, Imperial College London, South Kensington, London SW7 2AZ, UK*

GaAs based communications and optoelectronic devices are ubiquitous in everyday life. The growth of device structures by molecular beam epitaxy (MBE) underpins much of this technology. However, little is known about surface dynamics during MBE. This is chiefly because growth occurs under As2 or As4 flux which complicates the use of in situ, real-space imaging techniques.

Toward this end, we have developed a low energy electron microscope (LEEM) which combines surface electron microscopy with a III-V MBE system [1]. The incorporation of III-V MBE has necessitated significant modification to the basic LEEM system including the installation of multiple deposition sources, dedicated equipment for surface cleaning and an internal cooling shroud to limit the build-up of arsenic background pressure.

The new LEEM system has opened up the possibility of obtaining nanoscale movies of compound semiconductor surface dynamics. For example, we study the dynamics of Gallium droplets on GaAs(100) in Langmuir evaporation [2] with real-time imaging. Also, the dependency of congruent evaporation temperature on external As flux is investigated [3]. Finally, spectacular nucleation of 'daughter' droplets is observed during droplet coalescence which forms the basis for writing quantum structures [4]. It is promising that the III-V Surface Electron Microscope can further our understanding of III-V semiconductor growth mechanism in MBE.

[1] D. E. Jesson and W. X. Tang, *Surface Electron Microscopy of Ga Droplet Dynamics on GaAs (001)*, Microscopy: Science, Technology, Applications and Education" (Microscopy Book Series, number # 4), A. Méndez-Vilas (Editor), J. Díaz, Formatex (Badajoz, Spain), (in press).
[2] J. Tersoff, D. E. Jesson and W. X. Tang, *Science* **324** (2009) 236.
[3] Z. Y. Zhou, C. X. Zheng, W. X. Tang, D. E. Jesson and J. Tersoff, *Appl. Phys. Lett.* **97** (2010) 121912.
[4] J. Tersoff, D. E. Jesson and W. X. Tang, *Phys. Rev. Lett.* **105** (2010) 035702.

TP24

Spray Pyrolysis Prepared Hollow Spherical CuO/C: Synthesis, Characterization, and Its Application in Lithium-ion Batteries

C. Zhong, J.Z. Wang, S.L. Chou, K. Konstantinov and H.K. Liu

Institute for Superconducting and Electronic Materials, and ARC Center of Excellence for Electromaterials Science, University of Wollongong, NSW 2522, Australia

Copper oxide (CuO) is one of the most promising alternatives in lithium-ion battery anodes, with the theoretical capacity of 675 mAh g^{-1}. It also has the advantages of high safety, low cost and environment-friendly [1,2]. However, it suffers from poor cycling performance, which results from various factors, such as the large volume change and the serious agglomeration of the materials during the charge and discharge cycles. Carbon coating on the materials can be a very effective way to overcome these drawbacks [3]. Herein, a series of hollow spherical CuO-carbon materials were synthesized by an ultrafast one-step spray pyrolysis method using different furnace temperature and precursor concentration. The as-prepared materials were studied physically and electrochemically. Results demonstrate that carbon can be uniformly coated on the CuO hollow spheres by the spry pyrolysis method. Different furnace temperature and precursor concentration obviously affect the purity and morphology of the materials as well as its electrochemical performance.

[1] X. Zhang, G. Wang, X. Liu, H. Wu, *Mater. Chem. Phys.* **112**, 726 (2008).

[2] D. Majumdar, T.A. Shefelbine, T.T. Kodas, H.D. Glicksman, *J. Mater. Res.* **11**: 2861 (1996).

[3] S. Grugeon, S. Laruelle, R. Herrera-Urbina, L. Dupont, P. Poizot, J.M. Tarascon, *J. Electrochem. Soc.* **148**: A285 (2001).